Available online at www.sciencedirect.com
SCIENCE DIRECT®
ELSEVIER
International Journal of Solids and Structures 43 (2006) 2209–2242
INTERNATIONAL JOURNAL OF SOLIDS and STRUCTURES
www.elsevier.com/locate/ijsolstr

General non-linear finite element analysis of thick plates and shells

George Z. Voyiadjis *, Pawel Woelke

Department of Civil and Environmental Engineering, Louisiana State University, Baton Rouge, LA 70803-6405, USA

Received 23 December 2004; received in revised form 12 July 2005
Available online 30 August 2005

Abstract

A non-linear finite element analysis is presented, for the elasto-plastic behavior of thick shells and plates including the effect of large rotations. The shell constitutive equations developed previously by the authors [Voyiadjis, G.Z., Woelke, P., 2004. A refined theory for thick spherical shells. Int. J. Solids Struct. 41, 3747–3769] are adopted here as a base for the formulation. A simple C^0 quadrilateral, doubly curved shell element developed in the authors' previous paper [Woelke, P., Voyiadjis, G.Z., submitted for publication. Shell element based on the refined theory for thick spherical shells] is extended here to account for geometric and material non-linearities. The small strain geometric non-linearities are taken into account by means of the updated Lagrangian method. In the treatment of material non-linearities the authors adopt: (i) a non-layered approach and a plastic node method [Ueda, Y., Yao, T., 1982. The plastic node method of plastic analysis. Comput. Methods Appl. Mech. Eng. 34, 1089–1104], (ii) an Iliushin's yield function expressed in terms of stress resultants and stress couples [Iliushin, A.A., 1956. Plastichnost'. Gostekhizdat, Moscow], modified to investigate the development of plastic deformations across the thickness, as well as the influence of the transverse shear forces on plastic behaviour of plates and shells, (iii) isotropic and kinematic hardening rules with the latter derived on the basis of the Armstrong and Frederick evolution equation of backstress [Armstrong, P.J., Frederick, C.O., 1966. A mathematical representation of the multiaxial Bauschinger effect. (CEGB Report RD/B/N/731). Berkeley Laboratories. R&D Department, California.], and reproducing the Bauschinger effect. By means of a quasi-conforming technique, shear and membrane locking are prevented and the tangent stiffness matrix is given explicitly, i.e., no numerical integration is employed. This makes the current formulation not only mathematically consistent and accurate for a variety of applications, but also computationally extremely efficient and attractive.

Keywords: Thick plates and shells; Elasto-plastic analysis; Kinematic hardening; Large displacements

* Corresponding author. Tel.: +1 225 578 8668; fax: +1 225 578 9176.
E-mail address: voyiadjis@eng.lsu.edu (G.Z. Voyiadjis).

0020-7683/$ - see front matter © 2005 Elsevier Ltd. All rights reserved.
doi:10.1016/j.ijsolstr.2005.07.012

1. Introduction

Many approaches are used in the elasto-plastic analysis of plates and shells. The finite element method has been successful in modeling the linear behaviour of shells and it is therefore natural to apply the same method to the non-linear analysis of these technically important structures. Non-linear computations are based on incremental and/or iterative algorithms, which are computationally expensive. The efforts of many authors are not only directed to accuracy and wide applicability of their formulations, but also to computational efficiency. The objective of the present work is to develop a general, accurate and very efficient procedure for the analysis of thick/thin plates and shells, including geometric and material non-linearities with isotropic and kinematic hardening rules and an explicit form of the tangent stiffness matrix.

Many investigators avoid the problem of shell constitutive equations by following a layered approach, also referred to as 'through-the-thickness integration', (Dvorkin and Bathe, 1984; Flores and Onate, 2001; Kebari and Cassell, 1992; Kollmann and Sansour, 1997; Onate, 1999; Parish, 1981). This procedure, although accurate, requires sometimes prohibitively large storage of the computer. For the case of a non-layered finite element, a general and accurate shell theory is of crucial importance. Following the work of Voyiadjis and Shi (1991), Voyiadjis and Woelke (2004) presented a refined theory for thick shells, based on analytical closed form solutions for thick containers. This theory proves to be very efficient in the treatment of both thin and thick shells of general shape. It accounts for the effect of transverse shear deformation, distribution of radial stresses, as a very important feature for thick shells and the initial curvature effect. This not only contributes to the stress resultants and stress couples, but also results in a non-linear distribution of the in-plane stresses across the thickness of the shell. The resulting constitutive relations give very good results for extremely thick ($R/t = 3$), and very thin shells of general shape, as well as plates and beams. A brief outline of the theory is provided in subsequent sections.

The C^0 finite element given in Woelke and Voyiadjis (submitted for publication), based on the aforementioned theory, and the quasi-conforming technique, provides a very effective tool for elastic analysis of structures. The quasi-conforming technique given in Tang et al. (1980, 1983) is an extension of the assumed strain fields method (Ashwell and Gallagher, 1976; Huang and Hinton, 1984; Park and Stanley, 1986), and it has been successfully applied to overcome the locking phenomena (Shi and Voyiadjis, 1990, 1991). The biggest advantage of this technique, when compared with the most widely used selective integration method (Hughes, 1987; Stolarski and Belytschko, 1983; Stolarski et al., 1984; Yang et al., 2000; Zienkiewicz, 1978), is the fact that the stiffness matrix of the element is given explicitly. Thus, this method is very attractive for non-linear analysis where the element matrices are calculated many times during the analysis. Moreover, selective integration requires explicit segregation of transverse shear terms from bending and membrane terms, which is not possible when they are coupled, as is mostly the case for non-linear analysis. This problem was solved by a generalization of the selective integration procedure (Hughes, 1980). The quasi-conforming technique is however chosen here for its simplicity and low computational cost. As a result of this choice and the application of a non-layered approach, numerical integration will not be performed in the present procedure at any stage of the analysis. All the integrals are calculated analytically with the results later introduced into a computer code. This makes the current formulation consistent mathematically and extremely efficient from the point of view of computer time and power.

The strain fields are interpolated directly here, rather than obtained from the assumed displacement field providing the adequate representation of the rigid body modes. The spurious energy mode, which can be a problem in finite elements with reduced integration, is avoided here by the appropriate choice of the strain fields. The compatibility equations of the displacements can also be satisfied in the assumed strain fields. This results in a more complicated formulation of the element stiffness matrix, and therefore compatibility is not enforced. The element adopted in this work is unified for both curved and flat configurations, satisfies the Kirchhoff–Love hypothesis in the case of thin plates and shells, exhibits neither shear nor membrane locking and is free from spurious zero energy modes.

In elasto-plastic, finite element analysis of shells, large rotations and translations can play an important role. Displacements at the regions of the structure, which undergo inelastic deformations, can be very large. Thus, to achieve the desired accuracy, geometric non-linearities must be considered. The updated Lagrangian description, which has proven to be a very effective method (Bathe, 1982; Flores and Onate, 2001; Horrigmoe and Bergan, 1978; Kebari and Cassell, 1992) is adopted here. The element local coordinates and the local reference frame are continuously updated during the deformation. We consider large rotations and rigid translations here, but small strains with the total rotations decomposed into large rigid rotations and moderate relative rotations are also considered. The relative rotations and the derivatives of the in-plane displacements from two consecutive configurations can be considered small, (Shi and Atluri, 1988; Shi and Voyiadjis, 1991). Consequently, the quadratic terms of the derivatives of the in-plane displacement are negligible. We therefore have a non-linear analysis with large displacements and rotations but small strains. The transformation matrix given in Argyris (1982) is employed to handle large rigid rotations. The assumed strain finite element with an explicit form of the stiffness matrix, as described above, provides the linear part of the element tangent stiffness matrix.

Very many reliable 'layered models' for elasto-plastic analysis of shells have been published. In this approach, a plate or a shell is divided into layers where stresses are calculated and the yield condition is checked for each layer separately. The forces and moments are then calculated by integration through the thickness. Although this method can give very accurate results, it can also be very demanding in terms of computational power. If on the other hand a 'non-layered' approach is adopted, the yield function is integrated through the thickness of the plate or shell and therefore expressed in terms of stress resultants and couples. Numerical integration of the stresses is not necessary in this case, which makes the 'non-layered' formulation much cheaper computationally. The approximation of the yield criterion expressed in terms of forces and moments is expected to result in a loss of accuracy. This is however not the case as was shown by many authors comparing the two methods (Bieniek and Funaro, 1976; Owen and Hinton, 1980; Shi and Voyiadjis, 1992). Both models compare very well with the analytical solutions available in Hodge (1959), Olszak and Sawczuk (1977), Sawczuk (1989) and Sawczuk and Sokol-Supel (1993).

The non-layered model is employed in the current work with the yield function in terms of stress resultants and couples. In this case, the accuracy of the yield criterion is very important. A comparison of different yield surfaces can be found in Robinson (1971). A modified Iliushin's yield function is adopted in this work (Iliushin, 1956). Several modifications will be made to the original Iliushin's yield function.

The first modification allows for capturing the progressive development of the plastic curvatures across the thickness of the shell, as shown in Crisfield (1981) and Shi and Voyiadjis (1992). The model presented here very accurately reproduces the first yield point and tracks the growth of plastic curvatures until a plastic hinge is developed.

The transverse shear forces may significantly affect the plastic behaviour of both thick and, for certain loading conditions, thin shells. Shear becomes even more important in the case of anisotropic materials. Yet the influence of transverse shear forces on the plastic behaviour of plates and shells has been covered in the literature to a much lesser extent than in the case of elastic analysis, (Basar et al., 1992, 1993; Kratzig, 1992; Kratzig and Jun, 2003; Niordson, 1985; Noor and Burton, 1989; Palazotto and Linnemann, 1991; Reddy, 1989; Reissner, 1945). This effect is investigated here and it is shown that transverse shears influence strongly the plastic behaviour of considered structures.

Isotropic hardening as given in Shi and Atluri (1988) is also incorporated into the yield function in the present formulation. More importantly however, a kinematic hardening rule capable of capturing the Bauschinger effect is defined. It is well known that when a material or a structure is loaded in tension into a plastic zone, and subsequently the load is reversed, the yielding in compression will occur at a reduced value of stress. This anisotropy in the material is induced by plastic deformation. Relatively few hardening rules for non-layered plates and shells have been published that are capable of correctly representing this phenomenon. As first recognized by Wempner (1973), the stress resultants and couples of the classical

theory are not sufficient to describe accurately the state of stress in plastic shells. Bieniek and Funaro (1976) introduced 'hardening parameters', in the form of residual bending moments, allowing for the description of a Bauschinger effect. However, Bieniek and Funaro recognized that the 'hardening parameters' defined by them do not provide a full representation of kinematic hardening. For the appropriate representation of the rigid translation of the yield surface during non-elastic deformation in the stress resultant space, one needs not only the residual bending moments, but also residual shear and normal forces. These are equivalent parameters to the backstress in the stress space. We will therefore present a new kinematic hardening rule for non-layered plates and shells here, explicitly derived from the evolution of the backstress given by Armstrong and Frederick (1966). It is shown later that the approach presented here is very accurate, yet simple and efficient, which makes it very important form a practical engineering point of view.

Modeling of the elasto-plastic behaviour of structural elements based on the mathematical theory of plasticity involves analysis of spread of plastic deformations in the regions where the yield condition is satisfied. Alternatively, the inelastic deformations may be considered concentrated in the plastic hinges. The former method originates from the analytical limit analysis of structures performed under the assumption of elastic-perfectly plastic behaviour of the material (Hodge, 1959, 1963; Olszak and Sawczuk, 1977; Sawczuk and Sokol-Supel, 1993). Using the finite element method and the concept of the plastic hinges Ueda and Yao (1982) developed a 'plastic node method' for the plastic analysis of structures. In their formulation, the yield function is expressed in terms of stresses, as in the 'layered model'. Shi and Voyiadjis (1992) presented a non-layered plate element with the yield function in terms of forces and moments, adopting the concept of concentration of plastic deformations in the plastic hinges. A similar approach is adopted in this work, saving again computer time, yet giving very accurate results, as will be shown later.

This paper is divided into eight sections. After Section 1, the shell constitutive equations are briefly introduced. In Section 3, we present the shell kinematics. Section 4 is devoted to the linear element stiffness matrix. Section 5 gives a description of material non-linearities, with the definition of yield surface, flow and hardening rules. The elasto-plastic stiffness matrix of the element is derived in Section 6. In Section 7, we present an outline of a numerical procedure and a series of discriminating examples, demonstrating that the current computational model provides very good results for a variety of problems in elasto-plastic large displacement analysis of both thick and thin shells, plates and beams. Finally, in Section 8, we summarize the results and draw the conclusions.

2. Shell constitutive equations

Voyiadjis and Woelke (2004) presented a detailed derivation of the shell constitutive equations adopted for the finite element formulation. Only the final set of relations is given here for self-completeness. The refined theory accounts for the effect of transverse shear deformation, the distribution of radial stresses and the initial curvature of the shell, which results in a non-linear distribution of the in-plane stresses across the thickness of the shell.

The main features of the shell equations are the following:

(1) Assumed out of plane stress components that satisfy given traction boundary conditions. These are due to a closed form elasticity solution for thick walled spherical containers under internal and/or external uniform pressure, obtained by Lame (1852).
(2) Three-dimensional elasticity equations with an integral of the equilibrium equations.
(3) Stress resultants and stress couples acting on the middle surface of the shell together with average displacements along a normal of the middle surface of the shell and the average rotations of the normal (Voyiadjis and Baluch, 1981).

The membrane strains and curvatures in a rectangular coordinate system (x, y, z) are given by Eqs. (1)–(6).

$$\varepsilon_x = \frac{\partial u}{\partial x} + \frac{w}{R}, \tag{1}$$

$$\varepsilon_y = \frac{\partial v}{\partial x} + \frac{w}{R}, \tag{2}$$

$$\varepsilon_{xy} = \frac{1}{2}\left(\frac{\partial u}{\partial y} + \frac{\partial v}{\partial x}\right), \tag{3}$$

$$\kappa_x = \frac{\partial \phi_x}{\partial x} = \frac{\partial}{\partial x}\left(\frac{\partial w}{\partial x} - \gamma_{xz} - \frac{u}{R}\right), \tag{4}$$

$$\kappa_y = \frac{\partial \phi_y}{\partial y} = \frac{\partial}{\partial y}\left(\frac{\partial w}{\partial y} - \gamma_{yz} - \frac{v}{R}\right), \tag{5}$$

$$\kappa_{xy} = \frac{1}{2}\left(\frac{\partial \phi_x}{\partial y} + \frac{\partial \phi_y}{\partial x}\right), \tag{6}$$

where ε_x, ε_y, ε_{xy} are normal and shear strains and κ_x, κ_y, κ_{xy} are curvatures at the mid-surface in planes parallel to the xz, yz and xy planes respectively; u, v, w are the displacements along x, y, z axes respectively (Figs. 2 and 3); γ_{xz}, γ_{yz} are transverse shear strains in xz and yz planes (Fig. 1); ϕ_x, ϕ_y are angles of rotations of the cross-sections that were normal to the mid-surface of the undeformed shell (Figs. 1 and 4); R is a radius of the shell.

The stress resultants and couples M_x, M_y, M_{xy}, N_x, N_y, N_{xy}, Q_x, Q_y shown in Fig. 2, can be expressed in terms of the strains given above

$$M_x = D[\kappa_x + \nu\kappa_y], \tag{7}$$

$$M_y = D[\kappa_y + \nu\kappa_x], \tag{8}$$

$$M_{xy} = D(1-\nu)\kappa_{xy}, \tag{9}$$

$$N_x = S[\varepsilon_x + \nu\varepsilon_y], \tag{10}$$

$$N_y = S[\varepsilon_y + \nu\varepsilon_x], \tag{11}$$

$$N_{xy} = S(1-\nu)\varepsilon_{xy}, \tag{12}$$

$$Q_x = T\gamma_{xz}, \tag{13}$$

$$Q_y = T\gamma_{yz}, \tag{14}$$

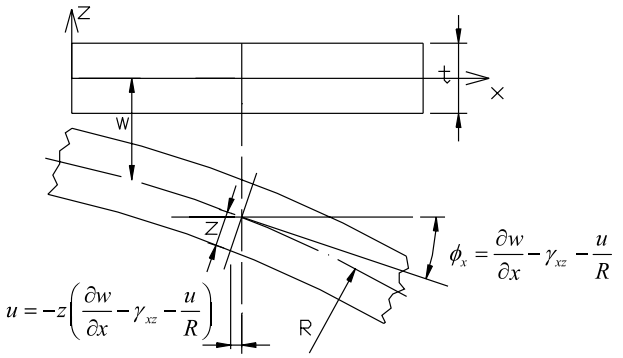

Fig. 1. Angle of rotation with transverse shear strains.

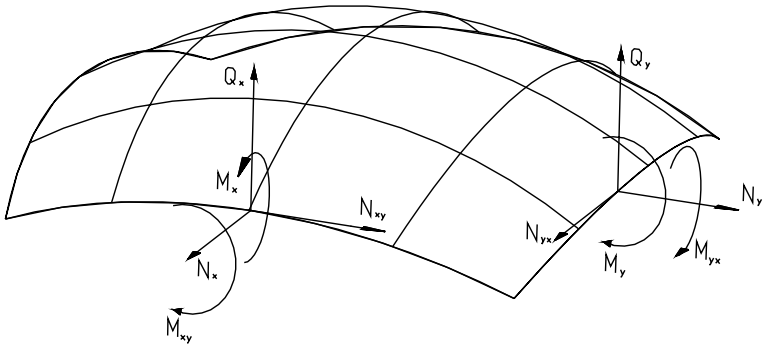

Fig. 2. Stress resultants on shell element.

where

$$D = \frac{Eh^3}{12(1-v^2)}, \quad S = \frac{Eh}{(1-v^2)}, \quad T = \frac{5}{12}\frac{Eh}{(1+v)} \tag{15}$$

and E is Young's Modulus, h is thickness of the shell, v is Poisson's ratio.

These constitutive equations reduce to those given by Flugge (1960) when the shear deformation and radial effects are neglected. We use the above equations to formulate the coupled strain energy density and derive the stiffness matrix of the element.

3. Shell kinematics

The updated Lagrangian method is employed in the present study of large displacements and rotations of the shell element. The coordinates of the nodal points are continuously updated during the deformation. The rotations are additively decomposed into large rigid rotations and moderate relative rotations (Shi and Voyiadjis, 1991).

The structure under consideration is defined in the global, fixed coordinate system **X**. We also have the local coordinate system **x**, surface coordinates at any nodal point $\mathbf{x}_s$, and base coordinates, which serve as a reference frame for the global degrees of freedom (Fig. 3).

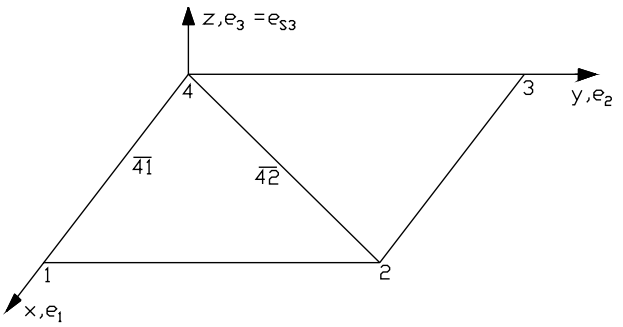

Fig. 3. Local coordinate system and normal vector $\mathbf{e}_{S3}$.

- Local coordinates

  In order to obtain the unit vector in the direction normal to the plane of the element, we first define two vectors, $\overrightarrow{41}$ and $\overrightarrow{42}$ connecting the origin of the coordinate system (point 4) to points 1 and 2 respectively. The cross product of these two vectors, divided by its length, gives $\mathbf{e}_3$, as shown in Fig. 3 and given by Eq. (16)

$$\mathbf{e}_3 = \frac{\overrightarrow{41} \times \overrightarrow{42}}{|\overrightarrow{41} \times \overrightarrow{42}|}. \tag{16}$$

  The unit vector $\mathbf{e}_2$ can be similarly obtained as a cross product of $\mathbf{e}_3$ and $\mathbf{e}_1$.We can now determine the relation between the global coordinates $\mathbf{X}$ and element local coordinates in configuration k

$$^k\mathbf{e} = {}^k\mathbf{R}\mathbf{E}, \tag{17}$$

  where $^k\mathbf{e}$ is the unit base vector of the local coordinates in configuration k, and $\mathbf{E}$ is the unit base vector of the global coordinates; $\mathbf{R}$ is a transformation matrix from local to global coordinates.

- Surface coordinates

  The surface coordinate system $\mathbf{x}_S$ originates at each node of the element. As defined by Shi and Voyiadjis (1991), the position and direction of this system are functions of rotations. Surface coordinates translate and rigidly rotate with the element. Consequently, $\mathbf{x}_{S3}$ is always normal to the surface of the element.The finite rigid body rotation vector $\mathbf{V}$ is given by

$$\mathbf{V} = \begin{bmatrix} \theta_1 \\ \theta_2 \\ \theta_3 \end{bmatrix}, \tag{18}$$

  where θ_1, θ_2, θ_3 are rigid body rotations around x, y, z axes respectively.The transformation matrix of large rotations $\mathbf{T}_\theta$, given by Argyris (1982) is used here

$$\mathbf{T}_\theta = \exp(\tilde{\theta}) \tag{19}$$

  with

$$\tilde{\theta} = \tilde{\theta}_{ij} = e_{ijk}\theta_k, \ k = 1,2,3, \tag{20}$$

  where $\tilde{\theta}$ is a skew symmetric matrix and e_{ijk} is the permutation tensor. In the above equation, the indicial notation is used with Einstein's summation convention. The transformation of the surface coordinates is therefore

$$\mathbf{V}' = \mathbf{T}_\theta \mathbf{V}, \tag{21}$$

  where $\mathbf{V}'$ is a rigid body rotation vector transformed into a new position. Similarly, we can write a transformation of the surface coordinates for a given rotation vector θ_j resulting from configuration $k-1$ to k at node j

$$^k\mathbf{e}_s = \mathbf{T}_{\theta j}^{k-1}\mathbf{e}_s, \tag{22}$$

  where $^k\mathbf{e}_s$ are the unit base vectors of the surface coordinates at configuration k. Defining the transformation between $\mathbf{E}$ and $^k\mathbf{e}_s$ as

$$^k\mathbf{e}_s = {}^k\mathbf{R}_s\mathbf{E} \tag{23}$$

  we can rewrite Eq. (22) as

$$^k\mathbf{e}_s = \mathbf{T}_{\theta j}^{k-1}\mathbf{R}_s\mathbf{E} = {}^k\mathbf{R}_s^k\mathbf{R}^{\mathrm{T}k}\mathbf{e} = {}^k\mathbf{S}_j{}^k\mathbf{e}, \tag{24}$$

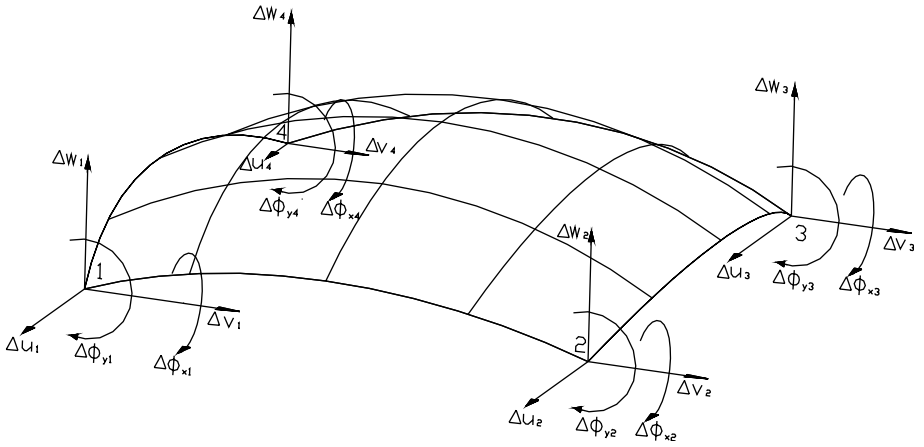

Fig. 4. Incremental degrees of freedom of shell element in local coordinates.

where ${}^{k}\mathbf{R}^{\mathrm{T}}$ is the transpose of ${}^{k}\mathbf{R}$ defined in Eq. (17) and ${}^{k}\mathbf{S}_j$ is a transformation matrix from local to the surface coordinate system. It is worthy to note that ${}^{0}\mathbf{R}_s$ is a 3×3 identity matrix for a flat plate.

- The base coordinates defined as by Horrigmoe and Bergan (1978) are adopted here as a common reference frame to which all element properties are transformed, prior to the assembly of the stiffness matrices. The base coordinates are defined by the combination of the fixed global and base coordinates.The global degrees of freedom at node j are the incremental translations: ΔU_j, ΔV_j, ΔW_j in directions of global coordinates X, Y, Z and rotations Θ_{xj}, Θ_{yj} around x_S, y_S. The local degrees of freedom at node j are the incremental translations Δu_j, Δv_j, Δw_j in directions of local coordinates x, y, z and rotations ϕ_{xj}, ϕ_{yj} around x, y. The transformation of the increments of the displacements at node j from the local coordinate system $\Delta\mathbf{q}_{\mathrm{e}j}$, to the corresponding base coordinates, $\Delta\mathbf{q}_{\mathrm{b}j}$ can be written as

$$\Delta\mathbf{q}_{\mathrm{b}j}=\begin{Bmatrix}\Delta U_j\\ \Delta V_j\\ \Delta W_j\\ \Theta_{xj}\\ \Theta_{yj}\end{Bmatrix}=\begin{bmatrix}{}^{k}\mathbf{R}^{\mathrm{T}} & 0\\ 0 & {}^{k}\mathbf{s}_j\end{bmatrix}\begin{Bmatrix}\Delta u_j\\ \Delta v_j\\ \Delta w_j\\ \phi_{xj}\\ \phi_{yj}\end{Bmatrix}={}^{k}\mathbf{T}_{\mathrm{b}j}\Delta\mathbf{q}_{\mathrm{e}j} \tag{25}$$

in which ${}^{k}\mathbf{s}_j$ is the upper left 2×2 submatrix of ${}^{k}\mathbf{S}_j$ defined in Eq. (24). The transformation matrix for the nodal displacement vector may be written as

$$\Delta\mathbf{q}_b={}^{k}\mathbf{T}_b\Delta\mathbf{q}_{\mathrm{e}}, \tag{26}$$

where ${}^{k}\mathbf{T}_b$ is composed of ${}^{k}\mathbf{T}_{\mathrm{b}j}$ with $j=1,2,3,4$.

The vector of the local increments of displacements nodal displacements is shown in Fig. 4 and given by Eq. (27)

$$\Delta\mathbf{q}_{\mathrm{e}j}=\{\Delta u_j,\Delta v_j,\Delta w_j,\Delta\phi_{xj},\Delta\phi_{yj}\}^{\mathrm{T}}\quad j=1,2,3,4. \tag{27}$$

4. Linear element stiffness matrix

An accurate and efficient shell finite element was presented in the authors' previous paper (Woelke and Voyiadjis, submitted for publication). It is an assumed strain type of element, free from locking and

spurious energy modes. The quasi-conforming technique (Tang et al., 1983) was used which gives an explicit form of the stiffness matrix as integrations are carried out directly. A detailed derivation is given in Woelke and Voyiadjis (submitted for publication).

In order to overcome the problem of shear locking, the Kirchhoff–Love assumption must be satisfied for the case of thin shells. Since the shear forces Q_x, Q_y are generally finite, the shear deformations γ_{xz} and γ_{yz} must vanish when the shear rigidity T approaches infinity. Hu (1984) point out that in order to satisfy this requirement the interpolation formulas must contain the ratio of the flexural and shear rigidities. We use here the approximation of the displacement w and rotations ϕ for the straight beam of length l given by Hu

$$w = \frac{1}{2}\left[1-\xi+\frac{\lambda}{2}(\xi^3-\xi)\right]w_i + \frac{1}{4}[1-\xi^2+\lambda(\xi^3-\xi)]\frac{l}{2}\phi_i + \frac{1}{2}\left[1+\xi-\frac{\lambda}{2}(\xi^3-\xi)\right]w_j + \frac{1}{4}[-1+\xi^2+\lambda(\xi^3-\xi)]\frac{l}{2}\phi_j, \tag{28}$$

$$\phi = -\frac{3}{2l}\lambda[1-\xi^2]w_i + \frac{1}{4}[2-2\xi-3\lambda(1-\xi^2)]\phi_i + + \frac{3}{2l}\lambda[1-\xi^2]w_j + \frac{1}{4}[2+2\xi-3\lambda(1-\xi^2)]\phi_j, \tag{29}$$

where

$$\xi = \frac{2x}{l} - 1 \leqslant \xi \leqslant 1; \quad \lambda = \frac{1}{\left(1+12\frac{D}{Tl^2}\right)}. \tag{30}$$

D and T denote the flexural and shear rigidity of the shell respectively. In equation, (30) the parameter D/Tl^2 accounts for the shear deformation effect. We notice that when shear rigidity is very large and $(h/l)^2 \to 0$, then $\lambda \to 1$, and w in Eq. (28) reduces to a Hermite function and the Kirchhoff–Love assumption is satisfied. When the shear rigidity is very small on the other hand, $\lambda = 0$, and Eq. (28) reduces to Cook's (1972) interpolation formula. The interpolation formulas given by Eqs. (28)–(30) are therefore suitable for both the classical theory of shells, as well as the thick shell theory based on which the present element is formulated.

The problem of membrane locking is avoided by the appropriate choice of the strain fields as well as a third order approximation of the membrane displacements u,v. Approximation of the strains independently of the displacements allows satisfying the inextensibility condition for very thin curved shells and thus any serious membrane locking is not experienced. Further details regarding overcoming shear and membrane locking may by found in Woelke and Voyiadjis (submitted for publication).

In the quasi-conforming technique, the displacement and strain fields are interpolated independently and the compatibility equations are only satisfied in a weak sense i.e., under the integral sign. The strain fields in the element are interpolated as follows:

- Linear bending strain field:

$$\boldsymbol{\varepsilon}_b = \begin{Bmatrix} \kappa_x \\ \kappa_y \\ 2\kappa_{xy} \end{Bmatrix} = \begin{Bmatrix} \frac{\partial \phi_x}{\partial x} \\ \frac{\partial \phi_y}{\partial y} \\ \frac{\partial \phi_x}{\partial y} + \frac{\partial \phi_y}{\partial x} \end{Bmatrix} = \begin{bmatrix} 1xyxy & & 0 \\ & 1xyxy & \\ 0 & & 1xy \end{bmatrix} \begin{Bmatrix} \alpha_1 \\ \alpha_2 \\ \alpha_3 \\ \dots \\ \alpha_{10} \\ \alpha_{11} \end{Bmatrix} = \mathbf{P}_b\boldsymbol{\alpha}_b. \tag{31}$$

- Stretch strain field:

$$\boldsymbol{\varepsilon}_{\mathrm{m}} = \begin{Bmatrix} \varepsilon_x \\ \varepsilon_y \\ 2\varepsilon_{xy} \end{Bmatrix} = \begin{Bmatrix} \dfrac{\partial u}{\partial x} + \dfrac{w}{R} \\ \dfrac{\partial v}{\partial y} + \dfrac{w}{R} \\ \dfrac{\partial u}{\partial y} + \dfrac{\partial v}{\partial x} \end{Bmatrix} = \begin{bmatrix} 1 & y & 0 & 0 & 0 \\ 0 & 0 & 1 & x & 0 \\ 0 & 0 & 0 & 0 & 1 \end{bmatrix} \begin{Bmatrix} \alpha_{12} \\ \alpha_{13} \\ \alpha_{14} \\ \alpha_{15} \\ \alpha_{16} \end{Bmatrix} = \mathbf{P}_{\mathrm{m}} \boldsymbol{\alpha}_{\mathrm{m}}. \tag{32}$$

- Constant transverse shear strain:

$$\boldsymbol{\varepsilon}_{\mathrm{s}} = \begin{Bmatrix} \gamma_{xz} \\ \gamma_{yz} \end{Bmatrix} = \begin{Bmatrix} \dfrac{\partial w}{\partial x} - \phi_x - \dfrac{u}{R} \\ \dfrac{\partial w}{\partial y} - \phi_y - \dfrac{v}{R} \end{Bmatrix} = \begin{bmatrix} 1 & 0 \\ 0 & 1 \end{bmatrix} \begin{Bmatrix} \alpha_{17} \\ \alpha_{18} \end{Bmatrix} = \mathbf{P}_{\mathrm{s}} \boldsymbol{\alpha}_{\mathrm{s}}, \tag{33}$$

where $\alpha_1, \alpha_2, \ldots, \alpha_{18}$, are the undetermined strain parameters.

Let $\mathbf{P}$ be the trial function for the assumed strain field i.e.,

$$\boldsymbol{\varepsilon} = \mathbf{P}\boldsymbol{\alpha} \tag{34}$$

and $\mathbf{N}$—the corresponding test function. We multiply both sides by the test function and integrate over the element domain

$$\int\int_{\Omega} \mathbf{N}^{\mathrm{T}} \boldsymbol{\varepsilon} \, \mathrm{d}\Omega = \boldsymbol{\alpha} \int\int_{\Omega} \mathbf{N}^{\mathrm{T}} \mathbf{P} \, \mathrm{d}\Omega. \tag{35}$$

The strain parameter $\boldsymbol{\alpha}$ is determined from the quasi-conforming technique as follows:

$$\boldsymbol{\alpha} = \mathbf{A}^{-1}\mathbf{C}\mathbf{q}, \tag{36}$$

where $\mathbf{q}$ is the element nodal displacement vector given by Eq. (27), and

$$\mathbf{A} = \int\int_{\Omega} \mathbf{N}^{\mathrm{T}} \mathbf{P} \, \mathrm{d}\Omega \quad \text{and} \quad \mathbf{C}\mathbf{q} = \int\int_{\Omega} \mathbf{N}^{\mathrm{T}} \boldsymbol{\varepsilon} \, \mathrm{d}\Omega. \tag{37}$$

The details of the evaluation of the $\mathbf{A}$, $\mathbf{C}$ matrices are given in Shi and Voyiadjis (1990), Shi and Voyiadjis (1991), Tang et al. (1983) and Woelke and Voyiadjis (submitted for publication). We may now express the strain field in terms of the nodal displacements as follows:

$$\boldsymbol{\varepsilon} = \mathbf{P}\boldsymbol{\alpha} = \mathbf{P}\mathbf{A}^{-1}\mathbf{C}\mathbf{q} = \mathbf{B}\mathbf{q}. \tag{38}$$

In most cases, it is convenient to take $\mathbf{P} = \mathbf{N}$ in order to obtain a symmetric stiffness matrix. This is the case in this work. Both matrices $\mathbf{A}$ and $\mathbf{C}$ may be easily evaluated explicitly. Illustration of this procedure is given in Tang et al. (1983) and Woelke and Voyiadjis (submitted for publication). We therefore obtain

$$\boldsymbol{\varepsilon}_{\mathrm{b}} = \mathbf{P}_{\mathrm{b}}\mathbf{A}_{\mathrm{b}}^{-1}\mathbf{C}_{\mathrm{b}}\mathbf{q} = \mathbf{B}_{\mathrm{b}}\mathbf{q} \tag{39}$$

$$\boldsymbol{\varepsilon}_{\mathrm{m}} = \mathbf{P}_{\mathrm{m}}\mathbf{A}_{\mathrm{m}}^{-1}\mathbf{C}_{\mathrm{m}}\mathbf{q} = \mathbf{B}_{\mathrm{m}}\mathbf{q} \tag{40}$$

$$\boldsymbol{\varepsilon}_{\mathrm{s}} = \frac{1}{\Omega}\mathbf{C}_{\mathrm{b}}\mathbf{q} = \mathbf{B}_{\mathrm{s}}\mathbf{q}, \tag{41}$$

where $\mathbf{B}_{\mathrm{b}}$, $\mathbf{B}_{\mathrm{m}}$, $\mathbf{B}_{\mathrm{s}}$ are the strain displacement matrices related to bending, stretch, transverse shear deformation respectively.

In order to determine the stiffness matrix of the element we make use of the strain energy density, expressed as follows:

$$U = \frac{1}{2}(M_x\kappa_x + M_y\kappa_y + 2M_{xy}\kappa_{xy} + N_x\varepsilon_x + N_y\varepsilon_y + 2N_{xy}\varepsilon_{xy} + Q_x\gamma_{xz} + Q_y\gamma_{yz}). \tag{42}$$

Substituting Eqs. (1)–(14) into the above expression and integrating over the element domain we obtain the following total strain energy Π_e in the element domain Ω

$$\Pi_e = \frac{1}{2}\int\int_{\Omega}(\boldsymbol{\varepsilon}_b^T\mathbf{D}\boldsymbol{\varepsilon}_b + \boldsymbol{\varepsilon}_m^T\mathbf{S}\boldsymbol{\varepsilon}_m + \boldsymbol{\varepsilon}_s^T\mathbf{T}\boldsymbol{\varepsilon}_s)\,d\Omega, \tag{43}$$

or using (39)–(41)

$$\Pi_e = \frac{1}{2}\mathbf{q}^T\int\int_{\Omega}(\mathbf{B}_b^T\mathbf{D}\mathbf{B}_b + \mathbf{B}_m^T\mathbf{S}\mathbf{B}_m + \mathbf{B}_s^T\mathbf{T}\mathbf{B}_s)\,d\Omega\mathbf{q}, \tag{44}$$

which leads to

$$\Pi_e = \frac{1}{2}\mathbf{q}^T[\mathbf{K}_b + \mathbf{K}_m + \mathbf{K}_s]\mathbf{q}, \tag{45}$$

where $\mathbf{K}_b$, $\mathbf{K}_m$, $\mathbf{K}_s$ are the element stiffness matrices related to bending, stretch and transverse shear deformation, given by

$$\mathbf{K}_b = \int\int_{\Omega}\mathbf{B}_b^T\mathbf{D}\mathbf{B}_b\,d\Omega, \tag{46}$$

$$\mathbf{K}_m = \int\int_{\Omega}\mathbf{B}_m^T\mathbf{S}\mathbf{B}_m\,d\Omega, \tag{47}$$

$$\mathbf{K}_s = \int\int_{\Omega}\mathbf{B}_s^T\mathbf{T}\mathbf{B}_s\,d\Omega. \tag{48}$$

The element stiffness matrix is then given by

$$\mathbf{K} = \mathbf{K}_b + \mathbf{K}_m + \mathbf{K}_s. \tag{49}$$

5. Yield criterion and hardening rule

As discussed in Section 1, a yield criterion in terms of stress resultants and couples is used here, similar to Iliushin's yield function. The yield function is modified to account for the progressive development of the plastic curvatures and shear forces, as given in Shi and Voyiadjis (1992). The Iliushin's yield function F can be written as

$$F = \frac{M^2}{M_0^2} + \frac{N^2}{N_0^2} + \frac{1}{\sqrt{3}}\frac{|MN|}{M_0N_0} - \frac{Y(k)}{\sigma_0^2} = 0, \tag{50}$$

or

$$F = \frac{|M|}{M_0} + \frac{N^2}{N_0^2} - \frac{Y(k)}{\sigma_0^2} = 0, \tag{51}$$

where

$$N^2 = N_x^2 + N_y^2 - N_x N_y + 3N_{xy}^2, \tag{52}$$

$$M^2 = M_x^2 + M_y^2 - M_x M_y + 3M_{xy}^2, \tag{53}$$

$$MN = M_x N_x + M_y N_y - \frac{1}{2}M_x N_y - \frac{1}{2}M_y N_x + 3M_{xy}^2, \tag{54}$$

$$M_0 = \frac{\sigma_0 h^2}{4}, \quad N_0 = \sigma_0 h \tag{55}$$

and σ_0 is the uniaxial yield stress, $Y(k)$ is a material parameter, which depends on isotropic hardening parameter k; h is the thickness of the shell, and $|\cdot|$ denotes absolute value.

The form of the yield condition given by Eq. (50), can be easily derived from the von Mises function and the definition of normal stresses at top and bottom surfaces of the shell, as shown in Bieniek and Funaro (1976). We can include the transverse shear forces Q_x, Q_y by modifying one of the stress intensities (Shi and Voyiadjis, 1992)

$$N^2 = N_x^2 + N_y^2 - N_x N_y + 3(N_{xy}^2 + Q_x^2 + Q_y^2). \tag{56}$$

It is shown later, (Examples 7.1 and 7.2) that the influence of the shear forces on plastic behaviour of thick plates and shells may be very important.

For a bending dominant situation, according to Eq. (50) or (51), the structure will behave linearly until the whole cross-section is plastic, i.e., the plastic hinge has formed. In reality however, the plastic curvature develops progressively from the outer fibers of the shell or plate and the material behaves non-linearly as soon as the outer fibers start to yield. To account for the development of plastic curvature across the thickness, Crisfield (1981) introduced a plastic curvature parameter $\alpha(\bar{\kappa}^p)$, into Eqs. (50) and (51)

$$F = \frac{M^2}{\alpha^2 M_0^2} + \frac{N^2}{N_0^2} + \frac{1}{\sqrt{3}\alpha}\frac{|MN|}{M_0 N_0} - \frac{Y(k)}{\sigma_0^2} = 0, \tag{57}$$

$$F = \frac{|M|}{\alpha M_0} + \frac{N^2}{N_0^2} - \frac{Y(k)}{\sigma_0^2} = 0, \tag{58}$$

where α was chosen such that αM_0 follows the uniaxial moment–plastic curvature relation:

$$\alpha = 1 - \frac{1}{3}\exp\left(-\frac{8}{3}\bar{\kappa}^p\right) \tag{59}$$

and

$$\bar{\kappa}^p = \sum \Delta\bar{\kappa}^p = \frac{Eh}{\sqrt{3}\sigma_0}\sum((\Delta\kappa_x^p)^2 + (\Delta\kappa_y^p)^2 + \Delta\kappa_x^p\Delta\kappa_y^p + (\Delta\kappa_{xy}^p)^2/4)^{1/2}. \tag{60}$$

$\bar{\kappa}^p$ is the equivalent plastic curvature, $\Delta\kappa_x^p$, $\Delta\kappa_y^p$ and $\Delta\kappa_{xy}^p$ are the increments of the plastic curvatures. We note that for $\bar{\kappa}^p = 0$, $\alpha = 2/3$ and we obtain $\alpha M_0 = \frac{\sigma_0 t^2}{6}$ which represents first fiber yielding. If on the other hand $\bar{\kappa}^p = \infty$, $\alpha = 1$ and we obtain fully plastic cross-section. Therefore, through the introduction of the plastic curvature parameter α we account for progressive development of the plastic curvatures and correctly predict the first yield.

To model the elasto-plastic behaviour of shells subjected to reversing loads, one needs a reliable kinematic hardening rule. Bieniek and Funaro (1976) introduced residual bending moments ('hardening parameters'), allowing for the description of the Bauschinger effect. These were later successfully applied for dynamic (Bieniek et al., 1976) and viscoplastic dynamic analysis of shells (Atkatsh et al., 1982, 1983). To determine correctly the rigid translation of the yield surface in the stress resultant space, we need not

only residual bending moments, but also residual normal and shear forces. These hardening parameters are related directly to the backstress, which represents the center of the yield surface in the stress space. We will therefore introduce a new kinematic hardening rule for plates and shells, with residual stress resultants, derived directly from the evolution of the backstress given by Armstrong and Frederick (1966). The yield surface is expressed as

$$F^* = \frac{|M^*|}{\alpha M_0} + \frac{(N^*)^2}{N_0^2} - \frac{Y(k)}{\sigma_0^2} = 0, \tag{61}$$

where

$$(N^*)^2 = (N_x - N_x^*)^2 + (N_y - N_y^*)^2 - (N_x - N_x^*)(N_y - N_y^*) + 3[(N_{xy} - N_{xy}^*)^2 + (Q_x - Q_x^*)^2 + (Q_y - Q_y^*)^2], \tag{62}$$

$$(M^*)^2 = (M_x - M_x^*)^2 + (M_y - M_y^*)^2 - (M_x - M_x^*)(M_y - M_y^*) + 3(M_{xy} - M_{xy}^*)^2, \tag{63}$$

where $M_x^*, M_y^*, M_{xy}^*, N_x^*, N_y^*, N_{xy}^*, Q_x^*, Q_y^*$ are above described residual bending moments, normal and shear forces respectively. We now proceed to definition of kinematic hardening parameters. For purpose of conciseness, we will use the indicial notation in the derivation, and only the final result will be given using engineering notation. The Armstrong and Frederick's evolution of the backstress ρ_{ij} is given by

$$\Delta\rho_{ij} = c\Delta\varepsilon_{ij}^p - a\rho_{ij}\Delta\varepsilon_{\text{eq}}^p, \tag{64}$$

where a and c are constants and the equivalent plastic strain increment is

$$\Delta\varepsilon_{\text{eq}}^p = \sqrt{\frac{2}{3}\Delta\varepsilon_{ij}^p\Delta\varepsilon_{ij}^p}. \tag{65}$$

The backstress represents the center of the transferred yield surface in the stress space. It has the dimension of stresses. To compute the stress resultants we need to integrate the stresses over the thickness of the plate. We will use the same definition here to derive hardening parameters, which represent the center of the yield surface in the stress resultant space. We therefore need to integrate the backstress over the thickness of the plate, to obtain residual normal and shear forces and bending moments. The definitions of the increments of hardening parameters are as follows:

$$\Delta N_{ij}^* = \int_{-h/2}^{h/2} \Delta\rho_{ij}\,\mathrm{d}z, \tag{66}$$

$$\Delta M_{ij}^* = \int_{-h/2}^{h/2} \Delta\rho_{ij} z\,\mathrm{d}z. \tag{67}$$

Substituting Eq. (64) into Eq. (66) we obtain

$$\Delta N_{ij}^* = \int_{-h/2}^{h/2} (c\Delta\varepsilon_{ij}^p - a\rho_{ij}\Delta\varepsilon_{\text{eq}}^p)\,\mathrm{d}z. \tag{68}$$

The increments of plastic strains $\Delta\varepsilon_{ij}^p$ in Eq. (68) are membrane strains, due to normal forces only. These are constant across the thickness of the shell, and we thus can write

$$\Delta N_{ij}^* = ch\Delta\varepsilon_{ij}^p - ah\rho_{ij}\Delta\varepsilon_{\text{eq}}^p. \tag{69}$$

Defining the hardening parameters similarly to stress resultants

$$h\rho_{ij} = N_{ij}^* \tag{70}$$

we can rewrite Eq. (69)

$$\Delta N^*_{ij} = ch\Delta\varepsilon^p_{ij} - aN^*_{ij}\Delta\varepsilon^p_{\mathrm{eq}}. \tag{71}$$

Constants a and c are given similarly to Bieniek and Funaro (1976)

$$a = c = \beta_1(1-F)\frac{1}{h}\frac{N_0}{\varepsilon_0}, \tag{72}$$

where N_0 and ε_0 are given by

$$N_0 = \sigma_0 h, \quad \varepsilon_0 = \sigma_0/E, \tag{73}$$

where F is a yield surface given in Eq. (58), h is a thickness of a plate and β_1 is a constant. We therefore obtain

$$\Delta N^*_{ij} = \beta_1(1-F)\frac{N_0}{\varepsilon_0}\left[\Delta\varepsilon^p_{ij} - \frac{1}{h}N^*_{ij}\Delta\varepsilon^p_{\mathrm{eq}}\right] \tag{74}$$

Similarly, substituting Eq. (64) into Eq. (67) we determine the increments of the residual bending moments

$$\Delta M^*_{ij} = \int_{-h/2}^{h/2}(c\Delta\varepsilon^p_{ij} - a\rho_{ij}\Delta\varepsilon^p_{\mathrm{eq}})z\,\mathrm{d}z, \tag{75}$$

where $\Delta\varepsilon^p_{ij}$ and $\Delta\varepsilon^p_{\mathrm{eq}}$ are

$$\Delta\varepsilon^p_{ij} = z\Delta\kappa^p_{ij}, \quad \Delta\varepsilon^p_{\mathrm{eq}} = \sqrt{\Delta\kappa^p_{ij}\Delta\kappa^p_{ij}}. \tag{76}$$

Substituting Eq. (76) into Eq. (75) and integrating it we have

$$\Delta M^*_{ij} = c\frac{h^3}{12}\Delta\kappa^p_{ij} - a\frac{h^3}{12}\rho_{ij}\Delta\kappa^p_{\mathrm{eq}}, \tag{77}$$

or

$$\Delta M^*_{ij} = c\frac{h^3}{12}\Delta\kappa^p_{ij} - a\frac{h}{2}M^*_{ij}\Delta\kappa^p_{\mathrm{eq}}, \quad \text{where } \rho_{ij}\frac{h^2}{6} = M^*_{ij} \tag{78}$$

and constants a and c are expressed similarly to those in Eq. (72)

$$a = c = \beta_2(1-F)\frac{12}{h^3}\frac{M_0}{\kappa_0}, \tag{79}$$

which leads to

$$\Delta M^*_{ij} = \beta_2(1-F)\frac{M_0}{\kappa_0}\left[\Delta\kappa^p_{ij} - \frac{6}{h^2}M^*_{ij}\Delta\kappa^p_{\mathrm{eq}}\right]. \tag{80}$$

The hardening parameters can now be rewritten in engineering notation

$$\text{If} \quad F^* = 1 \ \text{and} \ \nabla F^* > 0 \quad \text{(plastic loading)}$$

$$\Delta N^*_x = \beta_1(1-F)\frac{N_0}{\varepsilon_0}\left[\Delta\varepsilon^p_x - \frac{1}{h}N^*_x\Delta\varepsilon^p_{\mathrm{eq}}\right],$$

$$\Delta N^*_y = \beta_1(1-F)\frac{N_0}{\varepsilon_0}\left[\Delta\varepsilon^p_y - \frac{1}{h}N^*_y\Delta\varepsilon^p_{\mathrm{eq}}\right],$$

$$\Delta N^*_{xy} = \beta_1(1-F)\frac{N_0}{\varepsilon_0}\left[\Delta\varepsilon^p_{xy} - \frac{1}{h}N^*_{xy}\Delta\varepsilon^p_{\mathrm{eq}}\right], \tag{81}$$

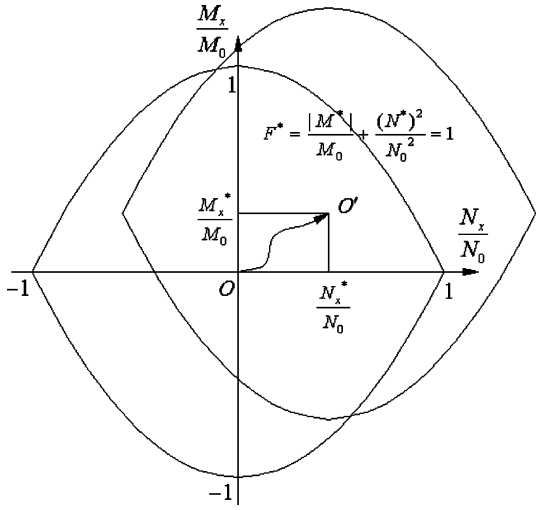

Fig. 5. Yield surface on N_xM_x plane —interpretation of kinematic hardening parameters O' is a center of transferred yield surface.

$$\Delta Q_x^* = \beta_1(1-F)\frac{N_0}{\varepsilon_0}\left[\Delta\varepsilon_{xz}^p - \frac{1}{h}Q_x^*\Delta\varepsilon_{\text{eq}}^p\right],$$
$$\Delta Q_y^* = \beta_1(1-F)\frac{N_0}{\varepsilon_0}\left[\Delta\varepsilon_{yz}^p - \frac{1}{h}Q_y^*\Delta\varepsilon_{\text{eq}}^p\right],$$
$$\Delta M_x^* = \beta_2(1-F)\frac{M_0}{\kappa_0}\left[\Delta\kappa_x^p - \frac{6}{h^2}M_x^*\Delta\kappa_{\text{eq}}^p\right],$$
$$\Delta M_y^* = \beta_2(1-F)\frac{M_0}{\kappa_0}\left[\Delta\kappa_y^p - \frac{6}{h^2}M_y^*\Delta\kappa_{\text{eq}}^p\right], \tag{82}$$
$$\Delta M_{xy}^* = \beta_2(1-F)\frac{M_0}{\kappa_0}\left[\Delta\kappa_{xy}^p - \frac{6}{h^2}M_{xy}^*\Delta\kappa_{\text{eq}}^p\right],$$

If $F^* < 1$ and $\nabla F^* \leqslant 0$ (unloading or neutral loading)

$$\Delta N_x^* = \Delta N_y^* = \Delta N_{xy}^* = \Delta Q_x^* = \Delta Q_y^* = \Delta M_x^* = \Delta M_y^* = \Delta M_{xy}^* = 0. \tag{83}$$

Parameters β_1 and β_2 in the above formulation control the membrane force–membrane strain and moment–curvature relations. A value $\beta_1 = \beta_2 = 2.0$ is found to be of sufficient accuracy in representation of behaviour of shells.

We therefore arrive at a final form of the yield function expressed in terms of stress resultants and couples with both isotropic and kinematic hardening rules. A graphic representation of yield surface given by (61) on the N_xM_x plane with $\alpha = 1$ and $Y = \sigma_0^2$ is shown in Fig. 5. Point O' denotes the transferred center of the yield surface.

6. Explicit tangent stiffness matrix

The plastic node method is adopted here, i.e., the plastic deformations are considered concentrated in the plastic hinges. The yield function is only checked at each node of the finite elements. If the combination of stress resultants satisfies the yield condition at a specific node, that node is considered plastic. Thus, in this

method the inelastic deformations are only considered at the nodes, while the interior of the element remains always elastic.

When node i of the element becomes plastic, the yield function takes the form

$$F_i^*(\mathbf{N}_i, \mathbf{Q}_i, \mathbf{M}_i, \mathbf{N}_i^*, \mathbf{Q}_i^*, \mathbf{M}_i^*, k) = 0, \tag{84}$$

where

$$\mathbf{N}_i = \begin{Bmatrix} N_x \\ N_y \\ N_{xy} \end{Bmatrix}, \quad \mathbf{Q}_i = \begin{Bmatrix} Q_x \\ Q_y \end{Bmatrix}, \quad \mathbf{M}_i = \begin{Bmatrix} M_x \\ M_y \\ M_{xy} \end{Bmatrix}, \quad \mathbf{N}_i^* = \begin{Bmatrix} N_x^* \\ N_y^* \\ N_{xy}^* \end{Bmatrix}, \quad \mathbf{Q}_i^* = \begin{Bmatrix} Q_x^* \\ Q_y^* \end{Bmatrix}, \quad \mathbf{M}_i^* = \begin{Bmatrix} M_x^* \\ M_y^* \\ M_{xy}^* \end{Bmatrix}. \tag{85}$$

At the same time the stress resultants must remain on the yield surface, i.e., the consistency condition must be satisfied

$$\frac{\partial F_i^*}{\partial \mathbf{M}_i} \mathrm{d}\mathbf{M}_i + \frac{\partial F_i^*}{\partial \mathbf{N}_i} \mathrm{d}\mathbf{N}_i + \frac{\partial F_i^*}{\partial \mathbf{Q}_i} \mathrm{d}\mathbf{Q}_i + \frac{\partial F_i^*}{\partial \mathbf{M}_i^*} \mathrm{d}\mathbf{M}_i^* + \frac{\partial F_i^*}{\partial \mathbf{N}_i^*} \mathrm{d}\mathbf{N}_i^* + \frac{\partial F_i^*}{\partial \mathbf{Q}_i^*} \mathrm{d}\mathbf{Q}_i^* + \frac{\partial F_i^*}{\partial k} \mathrm{d}\mathbf{k} = 0. \tag{86}$$

We assume an additive decomposition of strains into elastic and plastic parts

$$\varepsilon = \varepsilon^e + \varepsilon^p. \tag{87}$$

The associated flow rule is used here to determine the increments of plastic strains

$$\Delta\kappa_x^p = \sum_{i=1}^{\mathrm{NPN}} \Delta\lambda_i \frac{\partial F_i^*}{\partial M_{xi}}, \tag{88}$$

where NPN is the number of plastic nodes in the element and $d\lambda_i$ is a plastic multiplier. The remaining increments of the plastic strains are obtained in the same way. The plastic strain fields are interpolated as in linear elastic analysis (Eqs. (31)–(33)) rewritten here in the incremental form

$$\Delta\boldsymbol{\varepsilon}_{\mathrm{b}}^{\mathbf{p}} = \begin{Bmatrix} \Delta\kappa_x^p \\ \Delta\kappa_y^p \\ 2\Delta\kappa_{xy}^p \end{Bmatrix}, \quad \Delta\boldsymbol{\varepsilon}_{\mathrm{m}}^{\mathbf{p}} = \begin{Bmatrix} \Delta\varepsilon_x^p \\ \Delta\varepsilon_y^p \\ 2\Delta\varepsilon_{xy}^p \end{Bmatrix}, \quad \Delta\boldsymbol{\varepsilon}_{\mathrm{s}}^{\mathbf{p}} = \begin{Bmatrix} \Delta\gamma_{xz}^p \\ \Delta\gamma_{yz}^p \end{Bmatrix}. \tag{89}$$

The assumption of an additive decomposition of strains may be extended to displacements, provided that the strains are small (Shi and Voyiadjis, 1992; Ueda and Yao, 1982). Although geometric non-linearities are taken into account in the current work, we only consider large rigid rotations and translations, but small strains. Thus, we may write

$$q = q^e + q^p. \tag{90}$$

Following the work of Shi and Voyiadjis (1992) we approximate the increments of plastic displacements by the increments of plastic strains. The plastic rotation $\Delta\phi_x^p$ will be a function of both $\Delta\kappa_x^p$ and $\Delta\kappa_{xy}^p$, as can be deduced from Eq. (31). Assuming that increment of plastic nodal rotation $\Delta\phi_{xi}^p$ is proportional to the increment of elastic nodal rotation $\Delta\phi_{xi}$ we may express the former as

$$\Delta\phi_{xi}^p = \lim_{\delta\Omega\to 0} \int\int_{\partial\Omega_i} \left[\Delta\kappa_x^p + \frac{\Delta\phi_{xi}^2}{\Delta\phi_{xi}^2 + \Delta\phi_{yi}^2} 2\Delta\kappa_{xy}^p\right] \mathrm{d}x\,\mathrm{d}y = \Delta\lambda_i \left[\frac{\partial F_i^*}{\partial M_{xi}} + \frac{2\Delta\phi_{xi}^2}{\Delta\phi_{xi}^2 + \Delta\phi_{yi}^2} \frac{\partial F_i^*}{\partial M_{xyi}}\right], \tag{91}$$

where $\delta\Omega_i$ represents the infinitesimal neighborhood of node i. The vector of incremental nodal plastic displacements of the element at node i may then be expressed as

$$\Delta \mathbf{q}_i^{\mathbf{p}} = \mathbf{a}_i \Delta\lambda_i \tag{92}$$

with $\mathbf{a_i}$ given by

$$\mathbf{a}_i^{\mathrm{T}} = \left\{ \frac{\partial F_i^*}{\partial N_{xi}} + p_u \frac{\partial F_i^*}{\partial N_{xyi}}; \frac{\partial F_i^*}{\partial N_{yi}} + p_v \frac{\partial F_i^*}{\partial N_{xyi}}; \frac{\partial F_i^*}{\partial Q_{xi}} + \frac{\partial F_i^*}{\partial Q_{yi}}; \right.$$
$$\left. \frac{\partial F_i^*}{\partial M_{xi}} + p_{\phi x} \frac{\partial F_i^*}{\partial M_{xyi}}; \frac{\partial F_i^*}{\partial M_{yi}} + p_{\phi y} \frac{\partial F_i^*}{\partial M_{xyi}} \right\} \tag{93}$$

$$p_u = \frac{2\Delta u_i^2}{\Delta u_i^2 + \Delta v_i^2}; \quad p_v = \frac{2\Delta v_i^2}{\Delta u_i^2 + \Delta v_i^2}; \quad p_{\phi x} = \frac{2\Delta \phi_{xi}^2}{\Delta \phi_{xi}^2 + \Delta \phi_{yi}^2}; \quad p_{\phi y} = \frac{2\Delta \phi_{yi}^2}{\Delta \phi_{xi}^2 + \Delta \phi_{yi}^2}.$$

Eqs. (92) and (93) indicate that the plastic displacements at the nodes are only the functions of stress resultants at this node (Shi and Voyiadjis, 1992). Therefore, we can write the vector of increments of nodal plastic displacements, as follows:

$$\Delta \mathbf{q}^{\mathbf{p}} = \begin{bmatrix} \mathbf{a_1} & \mathbf{0} & \mathbf{0} \\ \mathbf{0} & \mathbf{a}_i & \mathbf{0} \\ \mathbf{0} & \mathbf{0} & \mathbf{a}_{\mathrm{NPN}} \end{bmatrix} \begin{Bmatrix} \Delta\lambda_1 \\ \Delta\lambda_i \\ \Delta\lambda_{\mathrm{NPN}} \end{Bmatrix} = \mathbf{a}\Delta\boldsymbol{\lambda}. \tag{94}$$

In order to determine the tangent stiffness matrix of the element we define $\delta\boldsymbol{\varepsilon}_{\mathrm{b}}$, $\delta\boldsymbol{\varepsilon}_{\mathrm{m}}$, $\delta\boldsymbol{\varepsilon}_{\mathrm{s}}$ as virtual elastic bending, membrane and transverse shear strains respectively (δ-virtual) and $\mathbf{M}, \mathbf{N}, \mathbf{Q}$ as stress couples and stress resultants of the element. We also make use of the linearized equilibrium equations of the system at configuration $k+1$ in the updated Lagrangian formulation, expressed by the principle of the virtual work, which in finite element modeling takes the form

$$\int_\Omega \int (\delta\boldsymbol{\varepsilon}_{\mathrm{b}}^{\mathrm{T}} \mathbf{D} \boldsymbol{\varepsilon}_{\mathrm{b}} + \delta\boldsymbol{\varepsilon}_{\mathrm{m}}^{\mathrm{T}} \mathbf{S} \boldsymbol{\varepsilon}_{\mathrm{m}} + \delta\boldsymbol{\varepsilon}_{\mathrm{s}}^{\mathrm{T}} \mathbf{T} \boldsymbol{\varepsilon}_{\mathrm{s}}) \,\mathrm{d}x\,\mathrm{d}y \int_\Omega \int \delta\boldsymbol{\theta}^{\mathrm{T}\,k} \mathbf{F} \boldsymbol{\theta} \,\mathrm{d}x\,\mathrm{d}y$$
$$= {}^{k+1}R - \int_\Omega \int (\delta\boldsymbol{\varepsilon}_{\mathrm{b}}^{\mathrm{T}\,k} \mathbf{M} + \delta\boldsymbol{\varepsilon}_{\mathrm{m}}^{\mathrm{T}\,k} \mathbf{N} + \delta\boldsymbol{\varepsilon}_{\mathrm{s}}^{\mathrm{T}\,k} \mathbf{Q}) \,\mathrm{d}x\,\mathrm{d}y, \tag{95}$$

where ${}^{k+1}R$ is the total external virtual work at step $k+1$ and $\boldsymbol{\theta}$ is the slope vector and ${}^{k}\mathbf{F}$ is a membrane stress resultant matrix at step k given by

$$\boldsymbol{\theta} = \begin{Bmatrix} \dfrac{\partial \Delta w}{\partial x} \\ \dfrac{\partial \Delta w}{\partial y} \end{Bmatrix}, \quad {}^{k}\mathbf{F} = \begin{bmatrix} {}^{k}N_x & {}^{k}N_{xy} \\ {}^{k}N_{xy} & {}^{k}N_{y}. \end{bmatrix} \tag{96}$$

The slope field $\boldsymbol{\theta}$ is evaluated in a similar way to the strain fields, using quasi-conforming technique (Tang et al., 1980, 1983). A bilinear interpolation is used as in Shi and Voyiadjis (1991) to approximate the slope field

$$\boldsymbol{\theta} = \begin{bmatrix} 1 & x & y & xy & 0 & 0 & 0 & 0 \\ 0 & 0 & 0 & 0 & 1 & x & y & xy \end{bmatrix} \begin{Bmatrix} \beta_1 \\ \beta_2 \\ \beta_3 \\ \beta_7 \\ \beta_8 \end{Bmatrix} = \mathbf{P}\boldsymbol{\beta} \tag{97}$$

with $\mathbf{P}$ denoting the trial function matrix and $\boldsymbol{\beta}$ is a vector of undetermined parameters, calculated in the same way as the vectors of strain parameters $\boldsymbol{\alpha}$ used to approximate the strain fields (Eqs. (31)–(33))

$$\boldsymbol{\beta} = \mathbf{A}^{-1}\mathbf{C}\Delta\mathbf{q}^{e}, \quad \mathbf{A} = \int_{\Omega}\int \mathbf{P}^{\mathrm{T}}\mathbf{P}\,\mathrm{d}x\,\mathrm{d}y, \quad \mathbf{C}\Delta\mathbf{q}^{e} = \int_{\Omega}\int \mathbf{P}^{\mathrm{T}}\boldsymbol{\theta}\,\mathrm{d}x\,\mathrm{d}y. \tag{98}$$

The details of the evaluation of the **A**, **C** matrices are given in Shi and Voyiadjis (1990), Shi and Voyiadjis (1991), Tang et al. (1983) and Woelke and Voyiadjis (submitted for publication). The slope field $\boldsymbol{\theta}$ is therefore expressed in terms of the slope–displacement matrix **G**

$$\boldsymbol{\theta} = \mathbf{P}\mathbf{A}^{-1}\mathbf{C}\Delta\mathbf{q}^{\mathbf{e}} = \mathbf{G}\Delta\mathbf{q}^{\mathbf{e}}. \tag{99}$$

The cubic interpolation of Δw along the boundary of the elements, given by Hu (1984) will be used here to evaluate **C** matrix

$$\begin{aligned}\Delta w(s) &= [1-\xi+\lambda(\xi-3\xi^2+2\xi^3)]\Delta w_i + [\xi-\xi^2+\lambda(\xi-3\xi^2+2\xi^2)]\frac{l_{ij}}{2}\Delta\phi_{si}\\ &\quad + [\xi-\lambda(\xi-3\xi^2+2\xi^3)]\Delta w_j + [-\xi+\xi^2+\lambda(\xi-3\xi^2+2\xi^2)]\frac{l_{ij}}{2}\Delta\phi_{sj},\\ \xi &= \frac{s}{l_{ij}}; \quad 0\leqslant s\leqslant l_{ij}; \quad 0\leqslant\xi\leqslant 1; \quad \lambda = \frac{1}{\left(1-12\frac{D}{TL^2}\right)},\end{aligned} \tag{100}$$

where l_{ij} is the distance between nodes i and j, $\Delta\phi_{si}$, $\Delta\phi_{sj}$ are tangential rotations at nodes i and j respectively, and D, T are flexural and transverse shear rigidities. The influence of parameter λ is explained in Hu (1984) and Woelke and Voyiadjis (submitted for publication).

Using Eq. (99), the virtual work principle given by (95) may now be rewritten

$$\begin{aligned}&\int_{\Omega}\int (\delta\boldsymbol{\varepsilon}_{\mathrm{b}}^{\mathrm{T}}\mathbf{D}\boldsymbol{\varepsilon}_{\mathrm{b}} + \delta\boldsymbol{\varepsilon}_{\mathrm{m}}^{\mathrm{T}}\mathbf{S}\boldsymbol{\varepsilon}_{\mathrm{m}} + \delta\boldsymbol{\varepsilon}_{\mathrm{s}}^{\mathrm{T}}\mathbf{T}\boldsymbol{\varepsilon}_{\mathrm{s}})\,\mathrm{d}x\,\mathrm{d}y + \delta\Delta\mathbf{q}^{e^{\mathrm{T}}}\mathbf{K}_{\mathrm{g}}\Delta\mathbf{q}^{e}\\ &\quad = {}^{k+1}R - \int_{\Omega}\int (\delta\boldsymbol{\varepsilon}_{\mathrm{b}}^{\mathrm{T}k}\mathbf{M} + \delta\boldsymbol{\varepsilon}_{\mathrm{m}}^{\mathrm{T}k}\mathbf{N} + \delta\boldsymbol{\varepsilon}_{\mathrm{s}}^{\mathrm{T}k}\mathbf{Q})\,\mathrm{d}x\,\mathrm{d}y,\end{aligned} \tag{101}$$

where $\mathbf{K}_{\mathrm{g}}$ is the initial stress matrix defined as

$$\mathbf{K}_{\mathrm{g}} = \int_{\Omega}\int \mathbf{G}^{\mathrm{T}k}\mathbf{F}\mathbf{G}\,\mathrm{d}x\,\mathrm{d}y \tag{102}$$

Substituting Eqs. (39)–(41) into the right-hand side of the above we can write

$$\int_{\Omega}\int (\delta\boldsymbol{\varepsilon}_{\mathrm{b}}^{\mathrm{T}k}\mathbf{M} + \delta\boldsymbol{\varepsilon}_{\mathrm{m}}^{\mathrm{T}k}\mathbf{N} + \delta\boldsymbol{\varepsilon}_{\mathrm{s}}^{\mathrm{T}k}\mathbf{Q})\,\mathrm{d}x\,\mathrm{d}y = \delta\Delta\mathbf{q}^{\mathrm{T}}\Delta\mathbf{f}, \tag{103}$$

where **f** is the internal force vector resulting from the unbalanced forces in configuration k and is expressed as follows:

$$\mathbf{f} = \int_{\Omega}\int (\mathbf{B}_{\mathrm{b}}^{\mathrm{T}k}\mathbf{M} + \mathbf{B}_{\mathrm{m}}^{\mathrm{T}k}\mathbf{N} + \mathbf{B}_{\mathrm{s}}^{\mathrm{T}k}\mathbf{Q})\,\mathrm{d}x\,\mathrm{d}y. \tag{104}$$

We may now rewrite Eq. (95) using Eqs. (7)–(14), written in a matrix form, and Eqs. (87), (104) as follows:

$$\int_{\Omega}\int \left[\left(\delta\boldsymbol{\varepsilon}_{\mathrm{b}}^{e^{\mathrm{T}}} + \delta\boldsymbol{\varepsilon}_{\mathrm{b}}^{p^{\mathrm{T}}}\right)\mathbf{M} + \left(\delta\boldsymbol{\varepsilon}_{\mathrm{m}}^{e^{\mathrm{T}}} + \delta\boldsymbol{\varepsilon}_{\mathrm{m}}^{p^{\mathrm{T}}}\right)\mathbf{N} + \left(\delta\boldsymbol{\varepsilon}_{\mathrm{s}}^{e^{\mathrm{T}}} + \delta\boldsymbol{\varepsilon}_{\mathrm{s}}^{p^{\mathrm{T}}}\right)\mathbf{Q}\right]\mathrm{d}x\,\mathrm{d}y + \delta\Delta\mathbf{q}^{e^{\mathrm{T}}}\mathbf{K}_{\mathrm{g}}\Delta\mathbf{q}^{e} = {}^{k+1}R - \delta\Delta\mathbf{q}^{\mathrm{T}}\Delta\mathbf{f} \tag{105}$$

rearranging terms and writing the above equation in incremental form

$$\int_{\Omega}\int\left(\delta\Delta\boldsymbol{\varepsilon}_{\mathrm{b}}^{e^{\mathrm{T}}}\Delta\mathbf{M}+\delta\Delta\boldsymbol{\varepsilon}_{\mathrm{m}}^{e^{\mathrm{T}}}\Delta\mathbf{N}+\delta\Delta\boldsymbol{\varepsilon}_{\mathrm{s}}^{e^{\mathrm{T}}}\Delta\mathbf{Q}\right)\mathrm{d}x\,\mathrm{d}y + \int_{\Omega}\int\left(\delta\Delta\boldsymbol{\varepsilon}_{\mathrm{b}}^{p^{\mathrm{T}}}\Delta\mathbf{M}+\delta\Delta\boldsymbol{\varepsilon}_{\mathrm{m}}^{p^{\mathrm{T}}}\Delta\mathbf{N}+\delta\Delta\boldsymbol{\varepsilon}_{\mathrm{s}}^{p^{\mathrm{T}}}\Delta\mathbf{Q}\right)\mathrm{d}x\,\mathrm{d}y+\delta\Delta\mathbf{q}^{e^{\mathrm{T}}}\mathbf{K}_{\mathrm{g}}\Delta\mathbf{q}^{e}={}^{k+1}R-\delta\Delta\mathbf{q}^{\mathrm{T}}\Delta\mathbf{f}. \tag{106}$$

Substituting Eq. (88) into Eq. (106) we obtain

$$\int_{\Omega}\int\left(\delta\Delta\boldsymbol{\varepsilon}_{\mathrm{b}}^{e^{\mathrm{T}}}\Delta\mathbf{M}+\delta\Delta\boldsymbol{\varepsilon}_{\mathrm{m}}^{e^{\mathrm{T}}}\Delta\mathbf{N}+\delta\Delta\boldsymbol{\varepsilon}_{\mathrm{s}}^{e^{\mathrm{T}}}\Delta\mathbf{Q}\right)\mathrm{d}x\,\mathrm{d}y + \sum_{i=1}^{\mathrm{NPN}}\delta\Delta\lambda_i\left[\frac{\partial F_i^*}{\partial\mathbf{M}_i}\mathrm{d}\mathbf{M}_i+\frac{\partial F_i^*}{\partial\mathbf{N}_i}\mathrm{d}\mathbf{N}_i+\frac{\partial F_i^*}{\partial\mathbf{Q}_i}\mathrm{d}\mathbf{Q}_i\right]+\delta\Delta\mathbf{q}^{e^{\mathrm{T}}}\mathbf{K}_{\mathrm{g}}\Delta\mathbf{q}^{e}={}^{k+1}R-\delta\Delta\mathbf{q}^{\mathrm{T}}\Delta\mathbf{f}. \tag{107}$$

Making use of the Eqs. (43)–(45), as well as the consistency condition given by Eq. (86), we may write

$$\delta\Delta\mathbf{q}^{e^{\mathrm{T}}}(\mathbf{K}+\mathbf{K}_{\mathrm{g}})\Delta\mathbf{q}^{e}-\sum_{i=1}^{\mathrm{NPN}}\delta\Delta\lambda_i\left[\frac{\partial F_i^*}{\partial\mathbf{M}_i^*}\mathrm{d}\mathbf{M}_i^*+\frac{\partial F_i^*}{\partial\mathbf{N}_i^*}\mathrm{d}\mathbf{N}_i^*+\frac{\partial F_i^*}{\partial\mathbf{Q}_i^*}\mathrm{d}\mathbf{Q}_i^*+\frac{\partial F_i^*}{\partial\mathbf{k}}\mathrm{d}\mathbf{k}\right]={}^{k+1}R-\delta\Delta\mathbf{q}^{\mathrm{T}}\Delta\mathbf{f}, \tag{108}$$

where $\mathbf{K}$ is the linear elastic stiffness matrix given by Eq. (49).

Similarly to Eq. (93) we define

$$\begin{aligned}\mathbf{a}_{\mathrm{b}i}^{\mathrm{T}}&=\frac{\partial F_i^*}{\partial\mathbf{M}_i^*}=\left\{\frac{\partial F_i^*}{\partial M_{xi}^*};\frac{\partial F_i^*}{\partial M_{yi}^*};\frac{\partial F_i^*}{\partial M_{xyi}^*}\right\},\\ \mathbf{a}_{\mathrm{m}i}^{\mathrm{T}}&=\frac{\partial F_i^*}{\partial\mathbf{N}_i^*}=\left\{\frac{\partial F_i^*}{\partial N_{xi}^*};\frac{\partial F_i^*}{\partial N_{yi}^*};\frac{\partial F_i^*}{\partial N_{xyi}^*}\right\},\\ \mathbf{a}_{\mathrm{s}i}^{\mathrm{T}}&=\frac{\partial F_i^*}{\partial\mathbf{Q}_i^*}=\left\{\frac{\partial F_i^*}{\partial Q_{xi}^*};\frac{\partial F_i^*}{\partial Q_{yi}^*}\right\}.\end{aligned} \tag{109}$$

Substituting Eq. (88) into Eqs. (81) and (82) we obtain

$$dM_x^*=\Delta M_x^*=\beta_2(1-F)\frac{M_0}{\kappa_0}\Delta\lambda\left[\frac{\partial F^*}{\partial M_x}-\frac{6}{h^2}M_x^*\sqrt{\frac{2}{3}\left[\left(\frac{\partial F^*}{\partial M_x}\right)^2+\left(\frac{\partial F^*}{\partial M_y}\right)^2+\left(\frac{\partial F^*}{\partial M_{xy}}\right)^2\right]}\right]. \tag{110}$$

Similar equations may be derived for the remaining hardening parameters. The vectors of hardening parameters will therefore yield

$$\mathrm{d}\mathbf{N}_i^*=\left\{\begin{array}{c}\Delta N_x^*\\ \Delta N_y^*\\ \Delta N_{xy}^*\end{array}\right\}=\Delta\boldsymbol{\lambda}\mathbf{A}_{\mathrm{m}i};\quad \mathrm{d}\mathbf{Q}_i^*=\left\{\begin{array}{c}\Delta Q_x^*\\ \Delta Q_y^*\end{array}\right\}=\Delta\boldsymbol{\lambda}\mathbf{A}_{\mathrm{s}i};\quad \mathrm{d}\mathbf{M}_i^*=\left\{\begin{array}{c}\Delta M_x^*\\ \Delta M_y^*\\ \Delta M_{xy}^*\end{array}\right\}=\Delta\boldsymbol{\lambda}\mathbf{A}_{\mathrm{b}i}, \tag{111}$$

where $\mathbf{A}_{\mathrm{m}i}$, $\mathbf{A}_{\mathrm{s}i}$, $\mathbf{A}_{\mathrm{b}i}$ are given by

$$\mathbf{A}_{\mathrm{m}i} = \left\{ \begin{array}{l} \beta_1(1-F)\dfrac{N_0}{\varepsilon_0}\left[\dfrac{\partial F^*}{\partial N_x} - \dfrac{1}{h}N_x^*\sqrt{\dfrac{2}{3}\left[\left(\dfrac{\partial F^*}{\partial N_x}\right)^2 + \left(\dfrac{\partial F^*}{\partial N_y}\right)^2 + \left(\dfrac{\partial F^*}{\partial N_{xy}}\right)^2\right]}\right], \\ \beta_1(1-F)\dfrac{N_0}{\varepsilon_0}\left[\dfrac{\partial F^*}{\partial N_y} - \dfrac{1}{h}N_y^*\sqrt{\dfrac{2}{3}\left[\left(\dfrac{\partial F^*}{\partial N_x}\right)^2 + \left(\dfrac{\partial F^*}{\partial N_y}\right)^2 + \left(\dfrac{\partial F^*}{\partial N_{xy}}\right)^2\right]}\right], \\ \beta_1(1-F)\dfrac{N_0}{\varepsilon_0}\left[\dfrac{\partial F^*}{\partial N_{xy}} - \dfrac{1}{h}N_{xy}^*\sqrt{\dfrac{2}{3}\left[\left(\dfrac{\partial F^*}{\partial N_x}\right)^2 + \left(\dfrac{\partial F^*}{\partial N_y}\right)^2 + \left(\dfrac{\partial F^*}{\partial N_{xy}}\right)^2\right]}\right] \end{array} \right\},$$

$$\mathbf{A}_{\mathrm{s}i} = \left\{ \begin{array}{l} \beta_1(1-F)\dfrac{N_0}{\varepsilon_0}\left[\dfrac{\partial F^*}{\partial Q_x} - \dfrac{1}{h}Q_x^*\sqrt{\dfrac{2}{3}\left[\left(\dfrac{\partial F^*}{\partial Q_x}\right)^2 + \left(\dfrac{\partial F^*}{\partial Q_y}\right)^2\right]}\right], \\ \beta_1(1-F)\dfrac{N_0}{\varepsilon_0}\left[\dfrac{\partial F^*}{\partial Q_y} - \dfrac{1}{h}Q_y^*\sqrt{\dfrac{2}{3}\left[\left(\dfrac{\partial F^*}{\partial Q_x}\right)^2 + \left(\dfrac{\partial F^*}{\partial Q_y}\right)^2\right]}\right] \end{array} \right\},$$

$$\mathbf{A}_{\mathrm{b}i} = \left\{ \begin{array}{l} \beta_2(1-F)\dfrac{M_0}{\kappa_0}\left[\dfrac{\partial F^*}{\partial M_x} - \dfrac{6}{h^2}M_x^*\sqrt{\dfrac{2}{3}\left[\left(\dfrac{\partial F^*}{\partial M_x}\right)^2 + \left(\dfrac{\partial F^*}{\partial M_y}\right)^2 + \left(\dfrac{\partial F^*}{\partial M_{xy}}\right)^2\right]}\right], \\ \beta_2(1-F)\dfrac{M_0}{\kappa_0}\left[\dfrac{\partial F^*}{\partial M_y} - \dfrac{6}{h^2}M_x^*\sqrt{\dfrac{2}{3}\left[\left(\dfrac{\partial F^*}{\partial M_x}\right)^2 + \left(\dfrac{\partial F^*}{\partial M_y}\right)^2 + \left(\dfrac{\partial F^*}{\partial M_{xy}}\right)^2\right]}\right], \\ \beta_2(1-F)\dfrac{M_0}{\kappa_0}\left[\dfrac{\partial F^*}{\partial M_{xy}} - \dfrac{6}{h^2}M_x^*\sqrt{\dfrac{2}{3}\left[\left(\dfrac{\partial F^*}{\partial M_x}\right)^2 + \left(\dfrac{\partial F^*}{\partial M_y}\right)^2 + \left(\dfrac{\partial F^*}{\partial M_{xy}}\right)^2\right]}\right] \end{array} \right\}. \tag{112}$$

Following the work of Shi and Voyiadjis (1992) we also define the isotropic hardening parameter as

$$\mathbf{H}\Delta\boldsymbol{\lambda} = \begin{bmatrix} H_1 & 0 & 0 \\ 0 & H_i & 0 \\ 0 & 0 & H_{\mathrm{NPN}} \end{bmatrix} \left\{ \begin{array}{c} \Delta\lambda_1 \\ \Delta\lambda_i \\ \Delta\lambda_{\mathrm{NPN}} \end{array} \right\} = -\left\{ \begin{array}{c} \dfrac{\partial F_1^*}{\partial k_1}dk_1 \\ \dfrac{\partial F_i^*}{\partial k_i}dk_i \\ \dfrac{\partial F_{\mathrm{NPN}}^*}{\partial k_{\mathrm{NPN}}}dk_{\mathrm{NPN}} \end{array} \right\}. \tag{113}$$

We may now substitute Eqs. (109), (111) and (113) into (108) to obtain

$$\delta\Delta\mathbf{q}^{e^{\mathrm{T}}}(\mathbf{K}+\mathbf{K}_{\mathrm{g}})\Delta\mathbf{q}^e + \delta\Delta\boldsymbol{\lambda}^{\mathrm{T}}\left[\mathbf{H} - \mathbf{a}_{\mathrm{b}}^{\mathrm{T}}\mathbf{A}_{\mathrm{b}} - \mathbf{a}_{\mathrm{m}}^{\mathrm{T}}\mathbf{A}_{\mathrm{m}} - \mathbf{a}_{\mathrm{s}}^{\mathrm{T}}\mathbf{A}_{\mathrm{s}}\right]\Delta\boldsymbol{\lambda} = {}^{k+1}R - \delta\Delta\mathbf{q}^{\mathrm{T}}\Delta\mathbf{f}, \tag{114}$$

or using (90) and (92)

$$\begin{aligned} &\left(\delta\Delta\mathbf{q}^{\mathrm{T}} - \delta\Delta\mathbf{q}^{p^{\mathrm{T}}}\right)(\mathbf{K}+\mathbf{K}_{\mathrm{g}})\Delta\mathbf{q}^e + \delta\Delta\boldsymbol{\lambda}^{\mathrm{T}}\left[\mathbf{H} - \mathbf{a}_{\mathrm{b}}^{\mathrm{T}}\mathbf{A}_{\mathrm{b}} - \mathbf{a}_{\mathrm{m}}^{\mathrm{T}}\mathbf{A}_{\mathrm{m}} - \mathbf{a}_{\mathrm{s}}^{\mathrm{T}}\mathbf{A}_{\mathrm{s}}\right]\Delta\boldsymbol{\lambda} - {}^{k+1}R + \delta\Delta\mathbf{q}^{\mathrm{T}}\Delta\mathbf{f} \\ &\quad = \delta\Delta\mathbf{q}^{\mathrm{T}}\left[(\mathbf{K}+\mathbf{K}_{\mathrm{g}})\Delta\mathbf{q}^e - {}^{k+1}R^* + \Delta\mathbf{f}\right] \\ &\qquad + \delta\Delta\boldsymbol{\lambda}^{\mathrm{T}}\left[-\mathbf{a}^{\mathrm{T}}(\mathbf{K}+\mathbf{K}_{\mathrm{g}})\Delta\mathbf{q}^e + \left(\mathbf{H} - \mathbf{a}_{\mathrm{b}}^{\mathrm{T}}\mathbf{A}_{\mathrm{b}} - \mathbf{a}_{\mathrm{m}}^{\mathrm{T}}\mathbf{A}_{\mathrm{m}} - \mathbf{a}_{\mathrm{s}}^{\mathrm{T}}\mathbf{A}_{\mathrm{s}}\right)\Delta\boldsymbol{\lambda}\right] = 0 \end{aligned} \tag{115}$$

with

$$^{k+1}R = {}^{k+1}R^{*}\delta\Delta\mathbf{q}. \tag{116}$$

By the virtue of the variational method Eq. (115) gives

$$\begin{aligned}&(\mathbf{K}+\mathbf{K}_{\mathrm{g}})\Delta\mathbf{q}^{e} - {}^{k+1}R^{*} + \Delta\mathbf{f} = 0\\ &-\mathbf{a}^{\mathrm{T}}(\mathbf{K}+\mathbf{K}_{\mathrm{g}})\Delta\mathbf{q}^{e} + \left(\mathbf{H} - \mathbf{a}_{\mathrm{b}}^{\mathrm{T}}\mathbf{A}_{\mathrm{b}} - \mathbf{a}_{\mathrm{m}}^{\mathrm{T}}\mathbf{A}_{\mathrm{m}} - \mathbf{a}_{\mathrm{s}}^{\mathrm{T}}\mathbf{A}_{\mathrm{s}}\right)\Delta\boldsymbol{\lambda} = 0.\end{aligned} \tag{117}$$

Substituting (90) and (92) into the above equations, we get

$$(\mathbf{K}+\mathbf{K}_{\mathrm{g}})\Delta\mathbf{q}^{e} - {}^{k+1}R^{*} + \Delta\mathbf{f} = (\mathbf{K}+\mathbf{K}_{\mathrm{g}})(\Delta\mathbf{q} - \mathbf{a}\Delta\boldsymbol{\lambda}) = {}^{k+1}R^{*} - \Delta\mathbf{f}, \tag{118}$$

$$-\mathbf{a}^{\mathrm{T}}(\mathbf{K}+\mathbf{K}_{\mathrm{g}})(\Delta\mathbf{q} - \mathbf{a}\Delta\boldsymbol{\lambda}) + \left(\mathbf{H} - \mathbf{a}_{\mathrm{b}}^{\mathrm{T}}\mathbf{A}_{\mathrm{b}} - \mathbf{a}_{\mathrm{m}}^{\mathrm{T}}\mathbf{A}_{\mathrm{m}} - \mathbf{a}_{\mathrm{s}}^{\mathrm{T}}\mathbf{A}_{\mathrm{s}}\right)\Delta\boldsymbol{\lambda} = 0. \tag{119}$$

Eq. (119) leads to

$$\Delta\boldsymbol{\lambda} = \left[\mathbf{a}^{\mathrm{T}}(\mathbf{K}+\mathbf{K}_{\mathrm{g}})\mathbf{a} + \left(\mathbf{H} - \mathbf{a}_{\mathrm{b}}^{\mathrm{T}}\mathbf{A}_{\mathrm{b}} - \mathbf{a}_{\mathrm{m}}^{\mathrm{T}}\mathbf{A}_{\mathrm{m}} - \mathbf{a}_{\mathrm{s}}^{\mathrm{T}}\mathbf{A}_{\mathrm{s}}\right)\right]^{-1}\mathbf{a}^{\mathrm{T}}(\mathbf{K}+\mathbf{K}_{\mathrm{g}})\Delta\mathbf{q}. \tag{120}$$

Eq. (118) becomes

$$\mathbf{K}_{\mathrm{epg}}\Delta\mathbf{q} = {}^{k+1}R^{*} - \Delta\mathbf{f}, \tag{121}$$

where $\mathbf{K}_{\mathrm{epg}}$ is the elasto-plastic, large displacement stiffness matrix of the element, given by

$$\mathbf{K}_{\mathrm{epg}} = (\mathbf{K}+\mathbf{K}_{\mathrm{g}})\left\{\mathbf{I} - \mathbf{a}\left[\mathbf{a}^{\mathrm{T}}(\mathbf{K}+\mathbf{K}_{\mathrm{g}})\mathbf{a} + \left(\mathbf{H} - \mathbf{a}_{\mathrm{b}}^{\mathrm{T}}\mathbf{A}_{\mathrm{b}} - \mathbf{a}_{\mathrm{m}}^{\mathrm{T}}\mathbf{A}_{\mathrm{m}} - \mathbf{a}_{\mathrm{s}}^{\mathrm{T}}\mathbf{A}_{\mathrm{s}}\right)\right]^{-1}\mathbf{a}^{\mathrm{T}}(\mathbf{K}+\mathbf{K}_{\mathrm{g}})\right\}. \tag{122}$$

The tangent stiffness matrix given by Eq. (122) is similar to the one presented by Shi and Voyiadjis (1992). The present formulation accounts for large displacements and consequently the stiffness matrix of the element contains the initial stress matrix $\mathbf{K}_{\mathrm{g}}$. More importantly however, the above derived stiffness matrix describes not only isotropic hardening, by means of parameter $\mathbf{H}$, but also kinematic hardening, through parameters $\mathbf{A}_{\mathrm{b}}$, $\mathbf{A}_{\mathrm{m}}$, $\mathbf{A}_{\mathrm{s}}$, which are not determined by curve fitting, but derived explicitly from the evolution equation of backstress given by Armstrong and Frederick (1966). We therefore have a non-layered finite element formulation with shell constitutive equations, yield condition, flow and hardening rules expressed in terms of membrane and shear forces and bending moments. All the variables used here, namely the stress resultants and couples, as well as the residual stress resultants and couples, representing the center of the yield surface, are derived from stresses and back-stresses in a very rigorous manner.

A very important feature of the derived tangent stiffness is its explicit form. The linear elastic stiffness matrix and initial stress matrix are determined by a quasi-conforming technique, which allows all the integrations to be performed analytically. The hardening parameters are also given explicitly. It is also noted that through the thickness integration is not employed here either, since the current model is the non-layered model with the yield condition expressed in terms of stress couples and resultants.

7. Numerical examples

For the purpose of the implementation of the model, a finite element code is developed in the programming language Fortran 90. A modified Newton–Raphson technique is employed to solve a system of nonlinear incremental equations. To overcome a singularity problem appearing at the limit point, the arc-length method (Crisfield, 1991) is adopted to determine the local load increment for each iteration. The return to the yield surface algorithm (Crisfield, 1991) is also implemented. The results delivered by

the current model are computed using a personal computer with AMD Athlon Processor, 1.8 GHz and 1.5 GB of RAM. Some of the reference solutions obtained with the layered approach (ABAQUS) were determined using a Silicon Graphics Onyx 3200 workstation.

The accuracy of the present formulation is verified through a series of discriminating examples. Since this paper is a continuation of the previous work of the authors (Woelke and Voyiadjis, submitted for publication), in which the linear elastic behavior of shells is examined, we will only solve non-linear examples here. The problems are chosen to challenge and demonstrate the most important features of the current model:

- Representation of the progressive development of plastic deformation until the plastic hinge is formed.
- The influence of the transverse shear forces on the plastic behavior of thick plates beams and shells of general shape.
- Elasto-plastic behaviour of structures of interest upon reversal of loading (representation of Bauschinger effect through kinematic hardening).
- Description of large displacements and rotations.

The performance of the proposed procedure is compared with other formulations available in the literature. Table 1 lists the references used here, and their corresponding abbreviations used later in the text.

7.1. Simply supported elasto-plastic beam

The importance of the transverse shear forces in the approximations of the collapse load of thick beams, plates and shells is known to be significant. Neglecting transverse shears in assessments of the maximum load carrying capacity of the structures may lead to predictions that are not conservative. Accurate and safe approximations should result in a decreasing value of the maximum load factor with increasing thickness. To test the accuracy of the current formulations in accounting for the shear deformation, we consider a simply supported beam of length $2L = 20$ in subjected to a concentrated load $2P = 20$ lbf at its mid-point. The Young's modulus is $E = 10.5E6$ psi, yield stress $\sigma = 500$ psi, and width of the beam is $b = 0.15$ in. We compute the load factor of the beam as a function of thickness. The analytical solution of this problem given by Hodge (1959) serves here as a reference solution.

As seen in Fig. 6, the current formulation agrees very well with analytical results of this problem by Hodge (1959). As expected we observe a substantial drop in the load factor for thick beams. We note, that for practical purposes only a certain range of H is significant. When the thickness of the beam, plate or shell

Table 1
Listing of the models used with abbreviations

Name	Description
ABQ-L	ABAQUS layered model with von Mises type yield criterion and Ziegler kinematic hardening rule (Hibbit, Karlson & Sorensen, Inc., 2001)
C&H	Bounds for collapse load—analytical solution of cylindrical shell Chen and Han (1988)
F&O	Numerical solution of pinched hemispherical shell by Flores and Onate (2001)
HOD	Analytical solution given by Hodge (1959)
O&HNL	Owen & Hinton non-layered model based on Mindlin plate theory and Iliushin's yield criterion (Owen and Hinton, 1980)
O&HL	Owen & Hinton Layered Model based on Mindlin plate theory and von Mises yield criterion (Owen and Hinton (1980))
SIMO	Numerical solution of pinched hemispherical shell by Simo et al. (1990)
V&W-Q	The present formulation with shear forces included in the yield function
V&W	The present formulation without shear forces included in the yield function

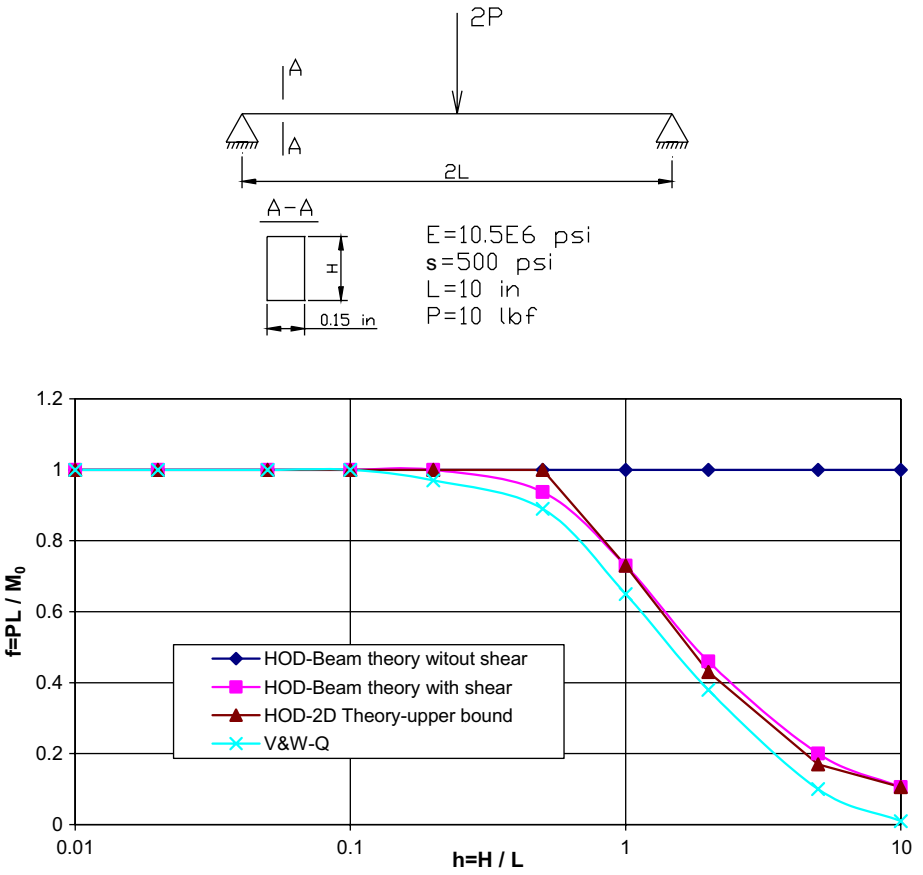

Fig. 6. Simply supported beam geometry, material properties and results: collapse load as a function of thickness.

reaches 50% of its total length, we clearly enter a purely academic problem, however still valuable for illustrational purposes.

The reduction of the load factor is very significant even for moderately thick beam i.e., $H = 0.5L$ (total length of the beam is $2L$), which is very closely approximated here.

7.2. Simply supported plate

The following example illustrates the accuracy of the current formulation in the prediction of the first yield in plates, as well as the description of the load–displacement response under cyclic loads. In this example, only material non-linearities will be examined, to allow for comparison with the reference solution by Owen and Hinton (1980).

We consider a square ($L = 1.0$ m) simply supported plate subjected to a uniformly distributed load $q = 1.0$ kPa. Young's modulus is $E = 10.92$ kPa, Poisson's ratio $v = 0.3$, yield stress $\sigma = 1600$ kPa and thickness of the plate $t = 0.01$ m. The geometry and material properties are shown in Fig. 7.

We compare the results obtained using the present finite element model with those published by Owen and Hinton (1980), with use of layered and non-layered model (O & HL, O & HNL—Table 1). The load–deflection responses are shown in Fig. 8.

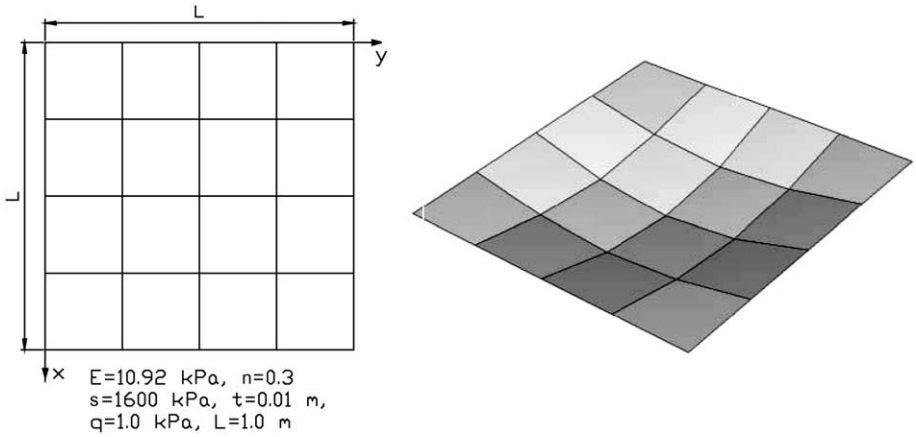

Fig. 7. Simply supported plate geometry, material properties and deformed shape.

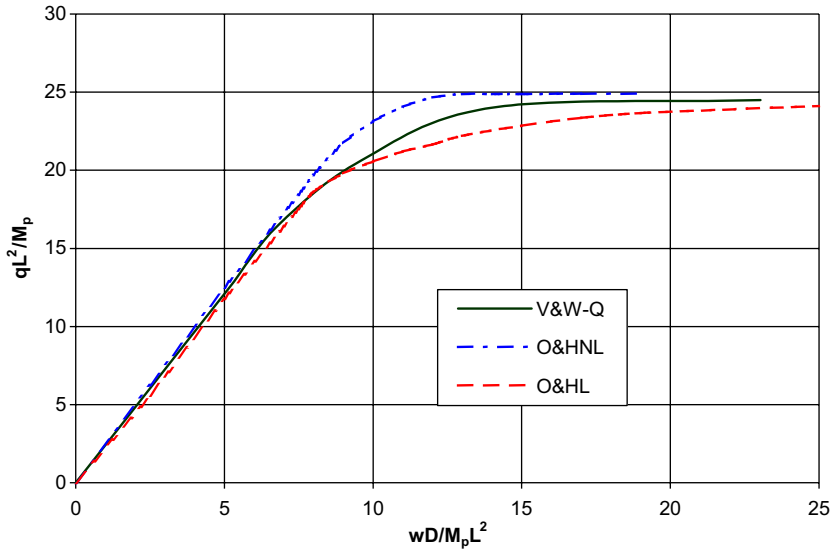

Fig. 8. Simply supported plate—load–displacement curves.

One of the objectives of the current work is to account for the progressive plasticization of the cross-section by means of a non-layered model. In a layered model, used here as a reference, we track the development of the plastic deformation directly, since stresses are calculated at several different levels (layers) in the model. In a layered model we operate in a stress resultant and stress couples space. The plastic bending moment is calculated under the assumption of fully plastic cross-section. Hence, typically the cross-section can only be either fully elastic or fully plastic, without any intermediate states. As seen in Fig. 8, the present approach provides a very good approximation of plastic strains growing gradually from outer fibers to the mid-plane.

The main thrust of this paper is developing a physically sound kinematic hardening rule for non-layered plates and shells, correctly representing not only the moment–curvature relationship, but also the normal forces–normal strain and the shear forces–shear strain relationships, upon complete reversal of loading.

We therefore need to show the importance of all hardening parameters $\mathbf{N}^*$, $\mathbf{Q}^*$, $\mathbf{M}^*$. The simply supported plate under a uniformly distributed load is a problem in which the normal forces are negligible. The residual forces $\mathbf{N}^*$ will then also be negligible. The influence of these is investigated in the following examples.

The current example is a bending dominant problem and hence the moment curvature relation is of primary importance. The load–displacement curve will take the shape of moment–curvature relation here. Fig. 9 shows the load–deflection curves for plate in Fig. 7, under reversed loading condition. The ABAQUS layered model with kinematic hardening rule is used here as a reference.

The current approximation is very close to the one of a layered approach, as seen in Fig. 9. This proves that the definition of residual bending moments $\mathbf{M}^*$ in the hardening rule is sound and produces accurate results. It is worthwhile to mention that the present model uses much less computational time and power than the layered approach because in the case of the latter the yield condition is checked at five layers across the thickness. This means that a computer program performs five times as many operations in the plastic zone as in the case of the current model. The number of layers increases with the increase of thickness of a shell. Thus, the present work is extremely valuable for the elasto-plastic analysis of thick plates, shells and beams.

For the thickness of the plate $t = 0.01$, the influence of the transverse shear forces on the plastic behavior is very small. In this case the residual transverse shear forces $\mathbf{Q}^*$ will not matter either. With increasing thickness of the plate, we observe increasing importance of the transverse shear forces as shown in Shi and Voyiadjis (1992). We will show here that for thick plates, both transverse shear forces and residual transverse shear forces play a very important role.

We consider the same rectangular simply supported plate as in Fig. 7. The thickness of the plate is however increased to $t = 0.35$ m, a uniform load to $q = 850$ kPa and the yield stress reduced to $\sigma = 1200$ kPa. The thickness of the plate is 35% of its length; hence we expect a significant reduction of the maximum load carried by the plate due to the influence of the shear forces. Again, we compare the results with the layered model, with the influence of transverse shears taken into account. The results are presented in Fig. 10.

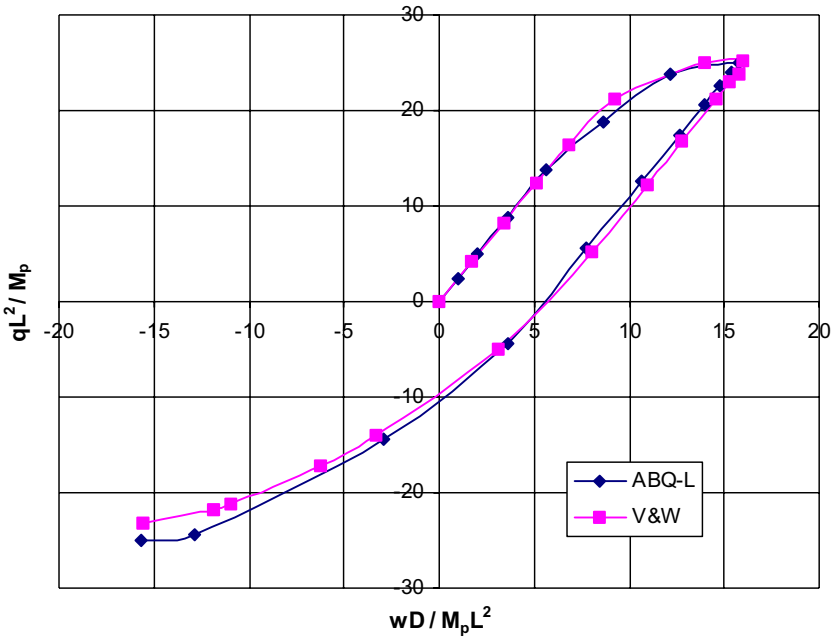

Fig. 9. Simply supported plate—Bauschinger effect.

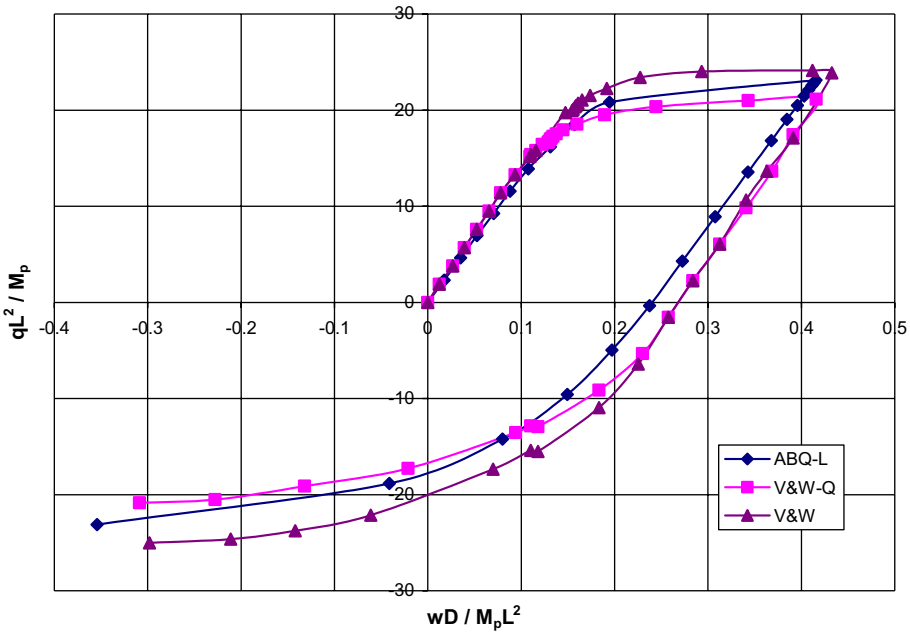

Fig. 10. Simply supported thick plate—Bauschinger effect.

A diamond line denoted by ABQ-L is a layered approach with shear forces considered. It serves here as a reference solution. We see that the current procedure performs very well is this test while at the same time being much more efficient.

As expected the influence of the shear forces on the approximations of the collapse load is significant. The analysis in which the transverse shear forces are not considered leads to a nearly 20% higher prediction of maximum load carried by the plate. Neglecting the shear forces when analyzing thick plates, shells and beams may lead to not conservative results.

When loading is reversed until yielding occurs at the top surface of the plate, the residual shear forces $\mathbf{Q}^*$ become important. The current model reproduces very well the lowered yield point upon reversal of loading, and offers a solution very close to the one of the layered approach. We therefore conclude that the representation of the residual shear forces as kinematic hardening parameters is physically sound and capable of delivering veracious results.

7.3. Cylindrical shell subjected to a ring of pressure

The previous example showed the validity of the definition of the residual bending moments and residual shear forces as kinematic hardening parameters. The derivation of the residual membrane forces is based on the same assumptions. Hence, we expect them to as reliable as the shear forces and bending moments. Since the membrane forces in bending of plates are negligible, the results of the former example do not prove that the formulation of the residual shear forces is sound. In order to do this, we investigate the cylindrical shell under the ring of pressure. The geometry, deformed shape of an octant of a cylinder and material parameters are shown in Fig. 11.

Due to symmetry we only need to consider an octant of a shell. The membrane forces play an important role here. If the structure is loaded into a plastic zone, then unloaded and loaded in the opposite direction,

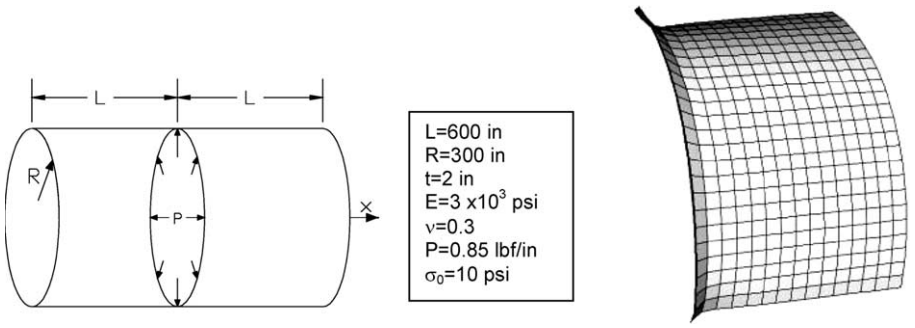

Fig. 11. Cylindrical shell subjected to a ring of pressure and a deformed shape.

the residual membrane forces also become noteworthy. The results of the analysis compared with the 'through-the-thickness integration' (layered) method are given in Fig. 12.

We recognize again that the present non-layered model with a new kinematic hardening rule is robust and agrees very well with the layered approach. The latter requires however five times as many operations for non-linear calculations, as the yield function and consistency condition need to be checked at each layer separately.

The problem presented here was originally investigated by Drucker (1954) and later by Chen and Han (1988) who analytically determined the bounds for the collapse load of the cylinder. These bounds are given by

$$1.5 \leqslant \frac{P}{\sigma_0 h \left(\frac{h}{R}\right)^{1/2}} \leqslant 2.0. \tag{123}$$

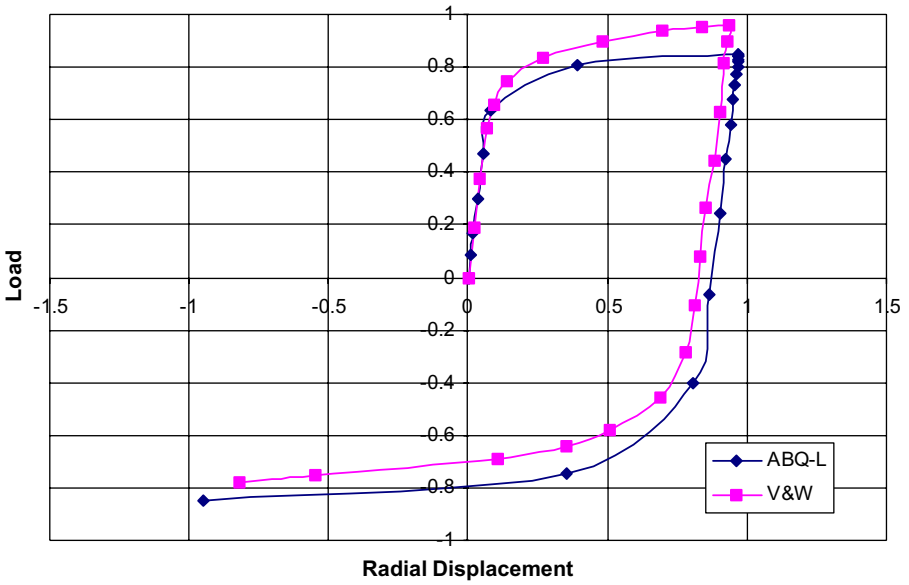

Fig. 12. Equilibrium path for a cylinder subjected to a ring of pressure.

The assessment of the collapse load of structures is of paramount importance from an engineering point of view. We therefore examine the functioning of this model in the determination of the maximum load carried by the cylinder. Eq. (123) will serve here as a reference solution. The collapse load as a function of thickness of the shell is given in Fig. 13.

It is seen that the predictions of the maximum load carried by the cylinder are accurate and falling within the analytical bounds. It is worthy to mention, that for the case of a very thick shells, the results approach the lower bound solution. This is due to the fact that the shear forces become more and more important for thick shells, causing reduction of the load carrying capacity.

7.4. Spherical dome with cut-out, subjected to a ring of pressure

A problem of a spherical dome with an 18° hole at the top, subjected to a ring of pressure will be solved here to establish a wide range of applicability of the method derived here. It is an important engineering problem, as well as a discriminating test of accuracy of the finite element representation of the behavior of shells. The performance of the yield function and kinematic hardening rule is studied here once again. The geometrical and material data are shown in Fig. 14.

The structure is loaded into a plastic zone, and then the pressure is reversed. The kinematic hardening rule is applied to determine the equilibrium path. The layered approach once again serves as a reference. The load–displacement curves are plotted in Fig. 15.

The approximation of the equilibrium path delivered by the current approach agrees very well with adopted reference solution, showing once again the validity of the assumptions made here. The lowered yield point is correctly reproduced by the yield surface defined in this paper.

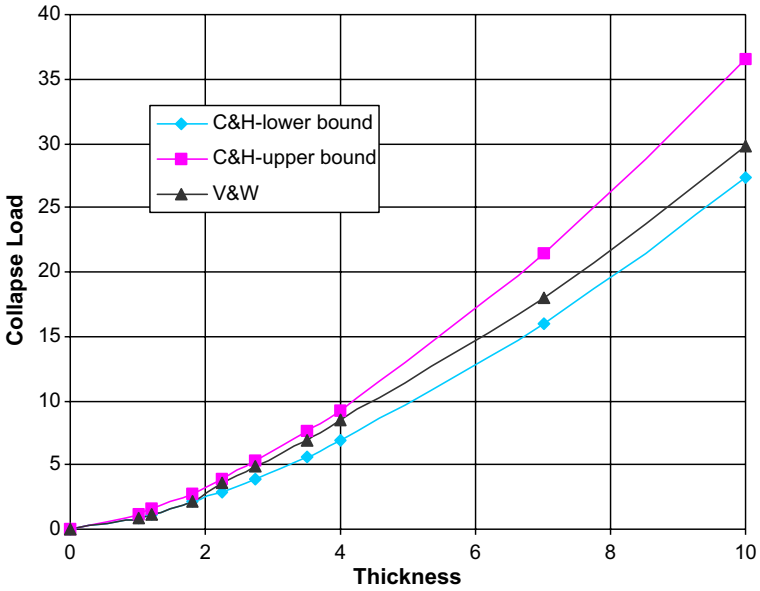

Fig. 13. Collapse load for a cylinder subjected to a ring of pressure.

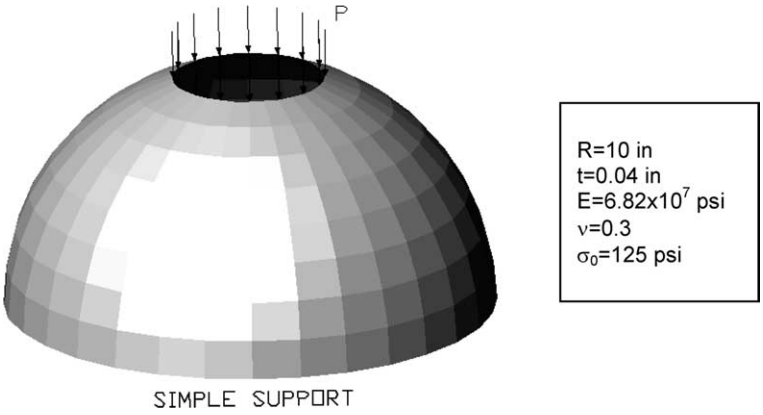

Fig. 14. Spherical dome with an 18° cut-out; geometry and material properties.

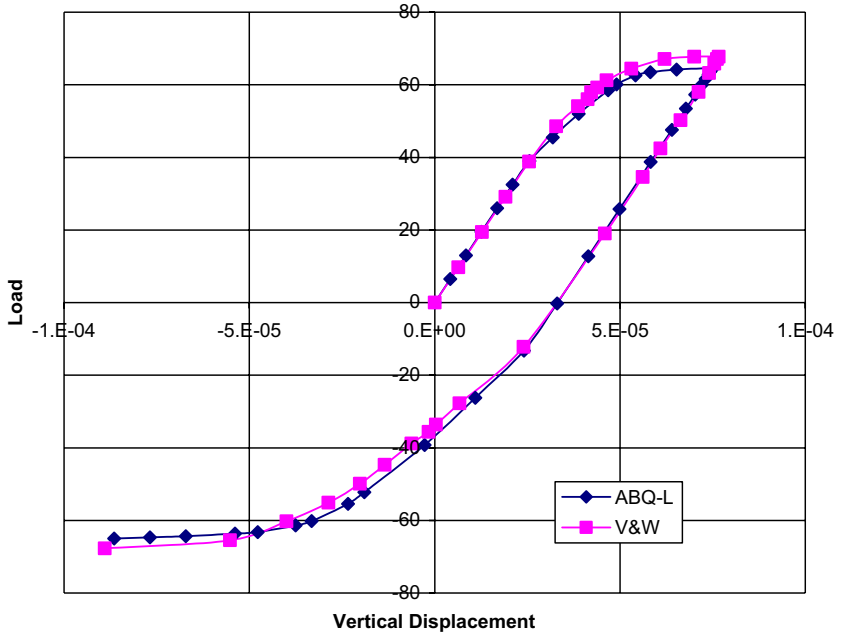

Fig. 15. Spherical dome with an 18° cut-out; load–displacement curves.

7.5. Pinched hemispherical shell–geometrically non-linear test

In order to demonstrate the adequacy of this work in the representation of large displacements (finite strains) we consider a popular benchmark problem–a pinched hemispherical shell (Morley Sphere), with an 18° hole at the top, subjected to four point loads alternating in sign at 90° intervals on the equator. Due to the symmetry, we only model a quadrant of the shell. The geometry, deformed shape and material properties are shown in Fig. 16.

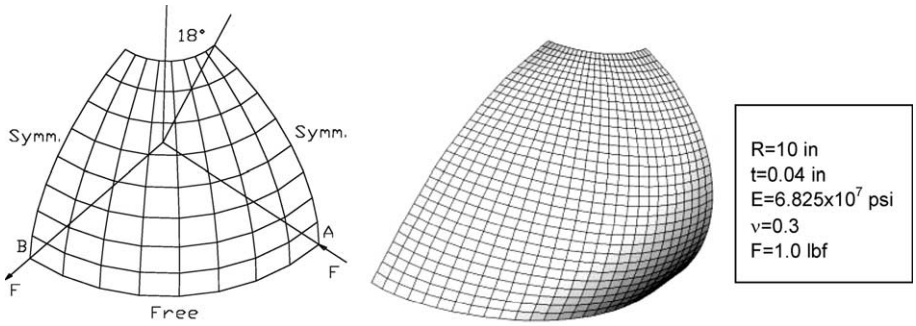

Fig. 16. Pinched hemispherical shell (Morley Sphere): geometry, deformed shape and material properties.

The elastic solution of the problem serves very often as a benchmark problem for the linear analysis of shells, (Belytschko et al., 1985; MacNeal and Harder, 1985; Morley and Morris, 1978; Simo et al., 1989; Woelke and Voyiadjis, submitted for publication). Ample sections of the shell rigidly rotate under these loading conditions, hence, precise modeling of the rigid body motion is essential for good performance in this test, (Belytschko et al., 1985). Simo et al. (1990) and also Parish (1995), Hauptmann and Schweizerhof (1998) and Flores and Onate (2001) used the same problem with an increased load factor to examine the capabilities of their models in the description of large deformation. We will only compare the results provided by the current formulation to those by Simo et al. and Flores et al. for conciseness. We note that in the case of a geometrically non-linear analysis, the deflections under alternating forces are not equal. We therefore plot the equilibrium path for both points of application of the load A and B. The load displacement path is plotted in Fig. 17.

The displacements calculated with V&W model (current model) compare very well with the reference solutions, proving that the present work gives adequate representation of large deformations.

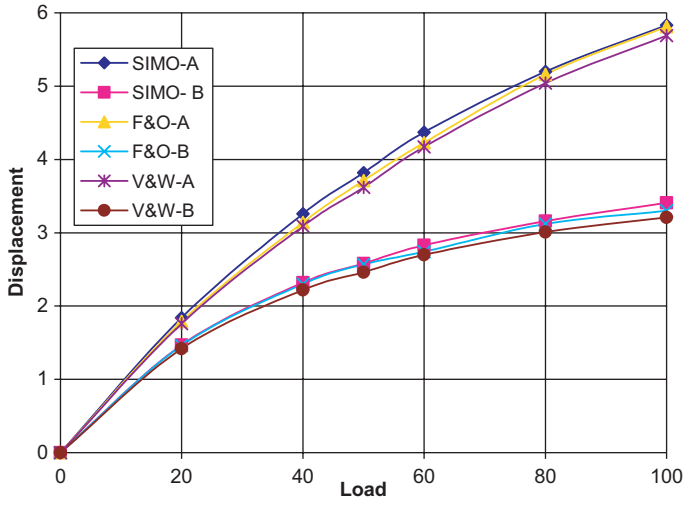

Fig. 17. Pinched hemispherical shell (Morley Sphere)—equilibrium paths (A—point under an inward load, B—point under an outward load).

8. Conclusions

A mathematically consistent finite element model for elasto-plastic, large rotations analysis of thin/thick shells is presented here. An accurate set of shell constitutive equations, previously developed by the same authors is adopted. The theory treats both thick and thin shells, with transverse shear deformation, radial stresses and initial curvature effects taken into account, which makes it accurate and reliable for a variety of applications.

A numerical implementation of the shell constitutive equations, by means of the 'quasi conforming technique', leads to the development of a finite element free from common deficiencies, i.e., shear and membrane locking and spurious energy modes. Moreover, integration is performed analytically, which is more precise from a mathematical point of view, and features an explicit form of the stiffness matrix. Numerical integration is not necessary which makes this formulation very efficient and attractive computationally.

The most important feature of the paper is the non-layered yield surface with a new kinematic hardening rule. Iliushin's yield function expressed in terms of stress resultants and couples, and modified to account for the progressive development of the plastic deformation and transverse shear forces is used. The kinematic hardening rule representing the rigid motion of the yield surface during loading, in the stress resultant space is also derived. It is capable of correctly determining the load–displacement response including the Bauschinger effect. Residual forces and bending moments are related to backstress using a similar definition to that of primary forces and moments. All the integrals are calculated analytically, which makes the current formulation extremely effective, as numerical integration is not employed at any stage of the computations. Thus, the kinematic hardening rule outlined here simplifies and speeds up the analysis, without any substantial loss of accuracy.

Large rotations and displacements are often associated with inelastic deformation. An updated Lagrangian method is utilized to describe the geometric non-linearities. We decompose rotations into large rigid rotations and moderate relative rotations. The strains are assumed to be small.

The reliability of the presented concept is numerically evaluated through a series of benchmark problems. In all the cases results are very close to the reference solutions, which demonstrates that the model is well grounded.

The effect of the shear forces on the plastic behavior and maximum load carrying capacity is correctly recognized. As expected, the results show a reduction of the limit load for thick plates, shells and beams, owing to the increasing significance of transverse shears.

The progressive plastification of the cross-section is also closely approximated. Typically, in the non-layered approach, the load displacement relation is linear until the plastic hinge is developed. Any yielding occurring before the section becomes fully plastic is neglected. Through a modification introduced by Crisfield (1981), the first yield of the outer fibers may be predicted as is also proven here.

The Bauschinger effect may only be numerically observed if the method employed features a veracious kinematic hardening rule. The one proposed here is defined in a stress resultant space, which is very effective from a structural analysis viewpoint. The lowered yield point upon reversal of load is correctly determined here for both plates and shells proving that the definition of the 'hardening parameters' is sound and capable of delivering very accurate results.

Example 7.5 evaluates the ability of the model to handle large rigid rotations. The solution offered here is once again precise demonstrating validity of large rotation formulation.

We note that although presented framework is robust for plates and shells of general shape, it performs best in the case of spherical shells. This is expected since the shell constitutive equations used here are derived by means of spherical strains, and later generalized through the finite element method.

The elastic analysis of shells by means of three-dimensional 'brick' elements is sometimes prohibitive due to the complexity of the problem. Shell elements are 'degenerated'; hence, they require a vastly reduced

number of operations executed by the computer. It allows engineers to predict the internal forces of complicated structures, which would have been difficult or impossible otherwise. Yet in the elasto-plastic considerations, most shell elements follow the layered approach, which is a concept similar to three dimensional 'brick' elements. While in the case of composite laminates, multi-layered shells give more accurate description of interlaminar effects, they lose their advantages in the analysis of isotropic homogenous shells. A non-layered method seems to be a natural consequence of the shell elements' development because the system of non-linear equations is expressed in terms forces and bending moments, and solved without discretization of the shell through the thickness. It allows taking the full advantage of shell elements in investigation of elasto-plastic behavior. A non-layered computational model consisting of a reliable shell element and a sound definition of the yield surface, isotropic and kinematic hardening rules capable of accurate description of elasto-plastic equilibrium path of shells under cyclic loading, is a great advancement.

The current work presents a complete and consistent formulation with redundant shell constitutive equations, finite element implementation in the elastic zone, yield surface and new kinematic hardening rule in the stress resultant space (non-layered method). It delivers very precise results of non-linear analysis of shells under cyclic loading, being at the same time simple and extremely effective.

The present model is also suitable for further enhancement leading to incorporation of damage effects, which will be shown in the next paper of the authors.

Acknowledgement

The authors gratefully acknowledge the help of Dr. P. Kattan who offered numerous valuable suggestions.

References

Argyris, J., 1982. An excursion into large rotations. Comput. Meth. Appl. Mech. Eng. 32, 85–155.

Armstrong, P.J., Frederick, C.O., 1966. A Mathematical Representation of the Multiaxial Bauschinger Effect. (CEGB Report RD/B/N/731). Berkeley Laboratories, R&D Department, California.

Ashwell, D.G., Gallagher, R.H. (Eds.), 1976. Finite Elements for Thin Shells and Curved Membranes. Wiley, New York.

Atkatsh, R.S., Bieniek, M.P., Sandler, I.S., 1982. Theory of viscoplastic shells for dynamic response. Technical report DNA-TR-81-50, Weidlinger Associates, New York.

Atkatsh, R.S., Bieniek, M.P., Sandler, I.S., 1983. Theory of viscoplastic shells for dynamic response. J. Appl. Mech. 50, 131–136.

Basar, Y., Ding, Y., Schultz, R., 1993. Refined shear-deformation models for composite laminates with finite rotations. Int. J. Solids Struct. 30 (19), 2611–2638.

Basar, Y., Ding, Y., Schultz, R., 1992. Shear-deformation models for the finite-rotation analysis of multilayered shell structures. Modeling of shells with non-linear behaviour, Euromech Colloquium 292, 2–4 September 1992, Munich, Germany.

Bathe, K.J., 1982. Finite Element Procedures in Engineering Analysis. Prentice-Hall, Englewood Cliffs, NJ.

Belytschko, T., Stolarski, H., Liu, W.K., Carpenter, N., Ong, J.S.-J., 1985. Stress projection for membrane and shear locking in shell finite elements. Comput. Methods Appl. Mech. Eng. 51, 221–258.

Bieniek, M.P., Funaro, J.R., 1976. Elasto-plastic behaviour of plates and shells. Technical report DNA 3584A, Weidlinger Associates, New York.

Bieniek, M.P., Funaro, J.R., Baron, M.L. 1976. Numerical analysis of the dynamic response of elasto-plastic shells. Technical report no. 20, November 1976, Weidlinger Associates, New York.

Chen, W., Han, D., 1988. Plasticity for Structural Engineers. Springer-Verlag, Berlin.

Cook, R.D., 1972. Two hybrid elements for analysis of thick and thin sandwich plates. Int. J. Numer. Methods Eng. 5, 277.

Crisfield, M.A., 1981. Finite element analysis for combined material and geometric nonlinearities. In: Wunderlich, W. (Ed.), Nonlinear Finite Element Analysis in Structural Mechanics. Springer-Verlag, New York, pp. 325–338.

Crisfield, M.A., 1991Non-linear Finite element Analysis of Solids and Structures, vol. 1. John Wiley & Sons Ltd., New York.

Drucker, D.C., 1954. Limit analysis of cylindrical shells under axially symmetric loading. In: Proc. 1st Midwestern Conf. Solid Mech., Urbana, Illinoi, pp. 158–163.

Dvorkin, E.N., Bathe, K.J, 1984. A continuum mechanics based four-node shell element for general non-linear analysis. Eng. Comput. 1, 77–88.
Flores, F.G., Onate, E., 2001. A basic thin shell triangle with only translational DOFs for large strain plasticity. Int. J. Numer. Methods Eng. 51, 57–83.
Flugge, W., 1960. Stresses in Shells. Springer, New York.
Hauptmann, R., Schweizerhof, K., 1998. A systematic development of 'solid-shell' element formulations for linear and non-linear analyses employing only displacement degrees of freedom. Int. J. Numer. Methods Eng. 42, 49–69.
Hibbit, Karlson & Sorensen, Inc. Abaqus, Theory Manual, Pawtucket, RI, USA.
Horrigmoe, G., Bergan, P.G., 1978. Nonlinear analysis of free form shells by flat elements. Comput. Methods Appl. Mech. Eng. 16, 11–35.
Hu, H.-C., 1984. Variational Principles of Theory of Elasticity with Applications. Scientific Publisher, Beijing, China.
Huang, H.C., Hinton, E., 1984. A nine-node Lagrangian plate element with enhanced shear interpolation. Eng. Comput. 1, 369–379.
Hughes, T.J.R., 1980. Generalization of selective integration procedures to anisotropic and nonlinear media. Int. J. Numer. Methods Eng. 15, 1413–1418.
Hughes, T.J.R., 1987. The Finite Element Method. Prentice-Hall, Englewood-Cliffs, NJ.
Hodge, P.G., 1959. Plastic Analysis of Structures. McGraw-Hill, NY.
Hodge, P.G., 1963. Limit Analysis of Rotationally Symmetric Plates and Shells. Prentice-Hall, Inc., Englewood Cliffs, NJ.
Iliushin, A.A., 1956. Plastichnost. Gostekhizdat, Moscow.
Kebari, H., Cassell, A.C., 1992. A stabilized 9-node non-linear shell element. Int. J. Numer. Methods Eng. 35, 37–61.
Kollmann, F.G., Sansour, C., 1997. Viscoplastic shells. Theory and numerical analysis. Arch. Mech. 49, 477–511.
Kratzig, W.B., 1992. 'Best' transverse shearing and stretching shelll theory for nonlinear finite element simulations. Comput. Methods Appl. Mech. Eng. 103, 135–160.
Kratzig, W.B., Jun, D., 2003. On 'best' shell models—From classical shells, degenerated and multi-layered concepts to 3D. Arch. Appl. Mech. 73, 1–25.
Lame, 1852. Lecons sur la theorie de l'elasticite. Paris, 1852.
MacNeal, H.R., Harder, R.L., 1985. A proposed standard set of problems to test finite element accuracy. Finite Element Anal. Des. 1, 3–20.
Morley, L.S.D., Morris, A.J., 1978. Conflict between finite elements and shell theory. Royal Aircraft Establishment Report, London.
Niordson, F.I., 1985. Shell Theory. North-Holland, Amsterdam.
Noor, A.K., Burton, W.S., 1989. Assessment of shear deformation theory for multilayered composite plates. Appl. Mech. Rev. 42 (1), 1–13.
Olszak, W., Sawczuk, A., 1977. Inelastic Behaviour in Shells. P. Noordhoff Ltd., Groningen, The Netherlands.
Onate, E., 1999. A review of some finite element families for thick and thin plate and shell analysis. In: Hughes, T.J.R., Onate, E., Zienkiewicz, O.C. (Eds.), Recent Developments in FE Analysis. CIMNE, Barcelona.
Owen, D.R.J., Hinton, E., 1980. Finite Elements in Plasticity: Theory and Practice. Pineridge Press, Swansea, UK.
Palazotto, A.N., Linnemann, P.E., 1991. Vibration and buckling characteristics of composite cylindrical panels incorporating the effects of a higher order shear theory. Int. J. Solids Struct. 28 (3), 341–361.
Parish, H., 1981. Large displacement of shells including material nonlinearties. Comput. Methods Appl. Mech. Eng. 27, 183–214.
Parish, H., 1995. A continuum-based shell theory for non-linear applications. Int. J. Numer. Methods Eng. 38, 1855–1883.
Park, K.C., Stanley, G.M., 1986. A curved C^0 shell element based on assumed natural coordinate strains. J. Appl. Mech. 53, 278–290.
Reddy, J.N., 1989. On refined computational models composite laminates. Int. J. Numer. Methods Eng. 27, 361–382.
Reissner, E., 1945. The effects of transverse shear deformation on the bending of elastic plates. J. Appl. Mech. ASME 12, 66–77.
Robinson, M., 1971. A comparison of yield surfaces for thin shells. Int. J. Mech. Sci. 13, 345–354.
Sawczuk, A., 1989. Mechanics and Plasticity of Structures. Polish Scientific Publishers, Warszawa.
Sawczuk, A., Sokol-Supel, J., 1993. Limit Analysis of Plates. Polish Scientific Publishers, PWN, Warszawa.
Shi, G., Atluri, S.N., 1988. Elasto-plastic large deformation analysis of space frames: a plastic-hinge and stress-based explicit derivation of tangent stiffnesses. Int. J. Numer. Methods Eng. 26, 589–615.
Shi, G., Voyiadjis, G.Z., 1990. A simple C^0 quadrilateral thick/thin shell element based on the refined shell theory and the assumed strain fields. Int. J. Solids Struct. 27 (3), 283–298.
Shi, G., Voyiadjis, G.Z., 1991. Simple and efficient shear flexible two node arch/beam and four node cylindrical shell/plate finite element. Int. J. Numer. Methods Eng. 31, 759–776.
Shi, G., Voyiadjis, G.Z., 1991. Efficient and accurate four-node quadrilateral C^0 plate bending element based on assumed strain fields. Int. J. Numer. Methods Eng. 32, 1041–1055.
Shi, G., Voyiadjis, G.Z., 1991. Geometrically nonlinear analysis of plates by assumed strain element with explicit tangent stiffness. Comput. Struct. 41, 757–763.
Shi, G., Voyiadjis, G.Z., 1992. A simple non-layered finite element for the elasto-plastic analysis of shear flexible plates. Int. J. Numer. Methods Eng. 33, 85–99.

Simo, J.C., Fox, D.D., Rifai, M.S., 1989. On a stress resultant geometrically exact shell model. Part II: The linear Theory. Comput. Methods Appl. Mech. Eng. 73, 53–92.

Simo, J.C., Fox, D.D., Rifai, M.S.., 1990. On a stress resultant geometrically exact shell model. Part III: Computational Aspects of the Nonlinear Theory. Comput. Methods Appl. Mech. Eng. 79, 21–70.

Stolarski, H., Belytschko, T., 1983. Shear and membrane locking in curved C^0 elements. Comput. Methods Appl. Mech. Eng. 41, 279–296.

Stolarski, H., Belytschko, T., Carpenter, N., Kennedy, J.M., 1984. A simple triangular curved shell element. Eng. Comput. 1, 210–218.

Tang, L., Chen, W., Liu, Y., 1980. Quasi conforming elements for finite element analysis. J. DIT 19 (2).

Tang, L., Chen, W., Liu, Y., 1983. String net function applications and quasi conforming technique. In: Hybrid Mixed Finite Element Methods. Wiley, NY.

Ueda, Y., Yao, T., 1982. The plastic node method of plastic analysis. Comput. Methods Appl. Mech. Eng. 34, 1089–1104.

Voyiadjis, G.Z., Baluch, H.M., 1981. Refined theory for flexural motions of isotropic plates. J. Sound Vib. 76, 57–64.

Voyiadjis, G.Z., Shi, G., 1991. Refined two-dimensional theory for thick cylindrical shells. Int. J. Solids Struct. 27, 261–282.

Voyiadjis, G.Z., Woelke, P., 2004. A refined theory for thick spherical shells. Int. J. Solids Struct. 41, 3747–3769.

Wempner, G.A., 1973. Nonlinear theory of shells. ASCE National Environmental Engineering Meeting, New York.

Woelke, P., Voyiadjis, G.Z., submitted for publication. Shell element based on the refined theory for thick spherical shells.

Yang, H.T.Y., Saigal, S., Masud, A., Kapania, R.K., 2000. A survey of recent shell finite elements. Int. J. Numer. Meth. Engng. 47, 101–127.

Zienkiewicz, O.C., 1978. The Finite Element Method. McGraw-Hill, NY.